Received: 23 October 2019 | Accepted: 28 March 2020

DOI: 10.1002/hyp.13770

WILEY

USING WATER AGE TO EXPLORE HYDROLOGICAL PROCESSES IN CONTRASTING ENVIRONMENTS

Multimodal water age distributions and the challenge of complex hydrological landscapes

Nicolas B. Rodriguez[1,2] | Paolo Benettin[3] | Julian Klaus[1]

[1]Catchment and Eco-Hydrology Research Group, Environmental Research and Innovation department, Luxembourg Institute of Science and Technology, Belvaux, Luxembourg

[2]Institute of Water Resources and River Basin Management, Karlsruhe Institute of Technology, Karlsruhe, Germany

[3]Laboratory of Ecohydrology ENAC/IIE/ECHO, École Polytechinque Fédérale de Lausanne, Lausanne, Switzerland

Correspondence
Nicolas B. Rodriguez, Catchment and Eco-Hydrology Research Group, Environmental Research and Innovation department, Luxembourg Institute of Science and Technology, Belvaux, Luxembourg.
Email: nicolas.bjorn.rodriguez@gmail.com

Funding information
École Polytechnique Fédérale de Lausanne; Fonds National de la Recherche Luxembourg, Grant/Award Numbers: FNR/CORE/C14/SR/8353440/STORE-AGE, FNR/CORE/C17/SR/11702136/EFFECT

Abstract

Travel time distributions (TTDs) are concise descriptions of transport processes in catchments based on water ages, and they are particularly efficient as lumped hydrological models to simulate tracers in outflows. Past studies have approximated catchment TTDs with unimodal probability distribution functions (pdf) and have successfully simulated tracers in outflows with those. However, intricate flow paths and contrasting water velocities observed in complex hydrological systems may generate multimodal age distributions. This study explores the occurrence of multimodal age distributions in hydrological systems and investigates the consequences of multimodality for tracer transport. Lumped models based on TTDs of varying complexity (unimodal and multimodal) are used to simulate tracers in the discharge of hydrological systems under well-known conditions. Specifically, we simulate tracer data from a controlled lysimeter irrigation experiment showing a multimodal response and we provide results from a virtual catchment-scale experiment testing the ability of a unimodal age distribution to simulate a known and more complex multimodal age system. Models are based on composite StorAge Selection functions, defined as weighted sums of pdfs, which allow a straightforward implementation of uni- or multi-modal age distributions while accounting for unsteady conditions. These two experiments show that simple unimodal models provide satisfactory simulations of a given tracer, but they fail in reproducing processes occurring at different temporal scales. Multimodal distributions, instead, can better capture the detailed dynamics embedded in the observations. We conclude that experimental knowledge of flow paths and the systematic use of data from multiple, independent tracers can be used to validate the assumption of water age unimodality. Multimodal age distributions are more likely to emerge in landscapes where the distributions of flow path lengths and/or water velocities are themselves multimodal. In general, age multimodality may not be particularly pronounced and detectable, unless comparable amounts of water with contrasting ages reach a given outflow.

KEYWORDS

hydrological tracer, lumped model, multimodal distribution, StorAge Selection function, travel time, water age distribution, water chemistry, water velocity

1 | INTRODUCTION

The representation of hydrological systems in mathematical terms is a challenging task that deals with the complexity of the natural environment (Bras, 2015; Clark et al., 2017; Dooge, 1986). Spatially implicit mathematical descriptions (e.g., lumped models) are widely used because they prove suitable to summarise hydrological processes at different scales (Hrachowitz & Clark, 2017). Transfer functions that relate system inputs to system outputs by an integral operation are particularly widespread in hydrology, notably for problems like flow and solute response of a catchment to precipitation events. Although the flow and solute responses are mathematically formulated with transfer functions in an almost identical way, the meaning of these functions is contrasting (Botter, Bertuzzo, & Rinaldo, 2010). The flow response deals with the celerity of pressure propagation, while the solute response deals with the velocity of water parcels within a catchment (Kirchner, Feng, & Neal, 2000; McDonnell & Beven, 2014).

Transfer functions are typically modelled as probability distribution functions (pdf) whose shape is assumed a priori and the relevant parameters are calibrated to available data. When focusing on the hydrological response of a catchment to an impulse input, the transfer function is termed instantaneous unit hydrograph (IUH) and its functional form is often assumed to be a gamma, lognormal or Weibull distribution. In some cases the shape of the IUH can be obtained starting from measurable properties of the landscape, such as its geomorphologic structure (Rinaldo, Marani, & Rigon, 1991; Rodriguez-Iturbe & Valdes, 1979). This type of unit hydrographs can have complex and multimodal shapes that originate from the geomorphological complexity of a catchment. Tracer hydrology focuses on the variations in the concentrations of non-ideal tracers like solutes (e.g., chloride) or ideal tracers like constituents of the water molecule (e.g., ^{2}H) that are transported with water. The transfer functions that are relevant to tracers (ideal or not) are termed travel (or transit) time distributions (TTD). These describe the time that water molecules take to move through a hydrological control volume (i.e., water ages in outflows) and they are used to relate tracer inputs (e.g., stable isotopes or chloride in precipitation) to tracer outputs (e.g., stable isotopes or chloride in discharge and evapotranspiration). Many studies employing TTDs as models of catchment transport have successfully simulated tracer concentrations in discharge by calibrating TTDs to tracer data under the assumption of steady-state flow conditions (see McGuire & McDonnell, 2006; Soulsby, Birkel, Geris, & Tetzlaff, 2015). TTDs are often assumed to be gamma-distributed because this shape is consistent with the spectral signatures of measured solute time series (Kirchner et al., 2000; Kirchner & Neal, 2013). Alternatively, various TTD shapes can be obtained by solving the advection–dispersion equation under different boundary conditions (Kreft & Zuber, 1978). These TTDs have been employed in groundwater systems with specific aquifer configurations (Małoszewski & Zuber, 1982). A comprehensive review of steady-state TTDs was provided by Leray, Engdahl, Massoudieh, Bresciani, and McCallum (2016), who illustrated the physical meaning and mathematical derivation of several TTD shapes.

If the assumption of steady-state flow conditions is removed (Botter et al., 2010; Botter, Bertuzzo, & Rinaldo, 2011), the resulting non-stationary TTDs are expected to have complex and irregular shapes even when the transport processes are simple (e.g., complete mixing). In transient hydrological conditions, the shape of non-steady TTDs cannot be assumed a priori, but StorAge Selection (SAS) functions (Botter et al., 2011; Harman, 2015; Rinaldo et al., 2015; van der Velde, Torfs, van der Zee, & Uijlenhoet, 2012) can be used to derive unsteady TTDs (also to derive steady-state TTDs in the particular case of steady flow conditions; Berghuijs & Kirchner, 2017). SAS functions can take different mathematical forms and have usually been assumed to be beta distributions (van der Velde et al., 2012; Visser et al., 2019), power functions (Benettin et al., 2017; Queloz et al., 2015) or gamma distributions (Harman, 2015; Wilusz, Harman, & Ball, 2017). The resulting unsteady TTDs display various peaks corresponding to the variability of the hydrological fluxes (i.e., precipitation or discharge). These TTDs may be called 'instantaneous' because they change at every moment due to temporal changes in water fluxes or to internal changes in the configuration of flow paths to the outlet (Kim et al., 2016). Yet, when 'instantaneous' TTDs are averaged out to obtain an average (or marginal) TTD, simple shapes emerge (Benettin, Soulsby, et al., 2017; Remondi, Kirchner, Burlando, & Fatichi, 2018; van der Velde et al., 2015) and suggest that it is still possible to approximate transport processes in a catchment with a single (marginal) TTD.

Whether TTDs are derived by direct calibration to data, by averaging unsteady TTDs starting from SAS functions, or by solving simplified fluid equations, their shape is often found/assumed to have a single mode. This seems to suggest that integrating a large number of contrasting flow paths results, on average, in a seamless distribution of transit times. But should we expect TTDs to always have simple shapes in the real world? And what processes can possibly give rise to multimodality in the TTD? Hydrological landscapes transport water inputs over a wide range of distances and in highly heterogeneous media with variable wetness conditions. It is unlikely that the existing plethora of transport processes always results in age distributions without multiple distinct and meaningful peaks. In fact, many studies (see Section 2) proposed to use multimodal age distributions in various hydrological systems for a number of physical reasons.

The problem of inferring the true shape of TTDs is made difficult by a major experimental issue: we cannot measure TTDs in catchments. TTDs can only be measured through tracer mass breakthrough curves, which is feasible in controlled systems like lysimeters (Pütz et al., 2016) or small experimental hillslopes (Kendall, McDonnell, & Gu, 2001; Kim et al., 2016; Rodhe, Nyberg, & Bishop, 1996; Volkmann et al., 2018). At the catchment scale, TTDs can only be deduced indirectly through aggregated tracer information in inflows and outflows (Kirchner, 2016). In other words, hypotheses about the TTDs (e.g., functional form and parameters) cannot be tested by comparing the assumed TTDs to actual measurements of water ages, but only by comparing the tracer simulation associated with the assumed TTD to the tracer observations. The task of deducing TTDs in catchments is often transformed into a model calibration problem and this may

overlook parts of the TTDs accounting for a range of transport processes not immediately visible in the tracer data (Figure 1). Until we are able to measure the true shape of an age distribution through a large-scale tracer experiment, research efforts are needed to assess the consequences of over-simplified age distributions. This is particularly important as TTDs are seen as a way to simulate solute chemistry and bridge previously disconnected fields of environmental modelling (Hrachowitz et al., 2016).

We first provide a reasonable definition of multimodality in the context of time-variable hydrological fluxes. Then, this study explores the occurrence of multimodal age distributions in hydrological systems and investigates the potential of lumped transport models to account for the causes and for the consequences of multimodality in tracer transport. We aim to clarify when we should expect to observe multimodal distributions in a hydrological system and what is the effect of not accounting for this multimodality.

The remainder of the article is organised as follows: Section 2 reviews previous studies that reported multimodal TTD behaviour. Section 3 reports the methodology to simulate tracer transport using TTDs and SAS functions. Section 4 provides modelling results for a lysimeter tracer experiment characterised by a bimodal tracer breakthrough curve, while Section 5 looks into the potential consequences of simplifying a multimodal TTD with a unimodal TTD by means of a catchment-scale virtual tracer experiment. A discussion of the results (Section 6) and a summary of the conclusions (Section 7) close the article.

2 | ACKNOWLEDGING THE MULTIMODALITY OF WATER AGE DISTRIBUTIONS

In various hydrological systems, TTDs are assumed to follow steady-state models such as the piston flow, the exponential and the dispersive models, or combinations of them (Małoszewski & Zuber, 1982). These analytical distributions work well in many catchments

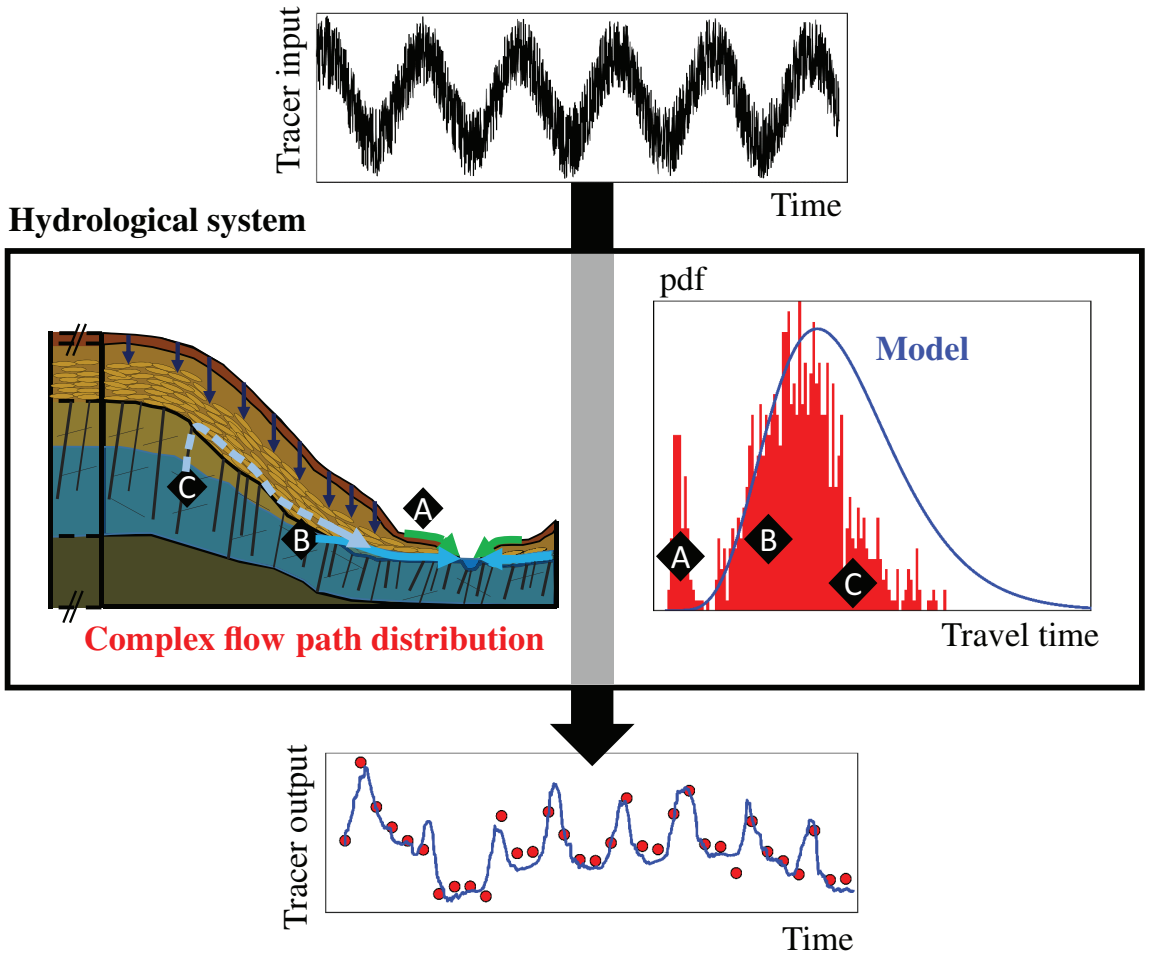

FIGURE 1 Visual summary of the process of modelling a hydrological system using lumped models based on TTDs and tracer input–output relationships. The complexity of discharge generation processes (a–c) results in multimodal TTDs (red histogram). (a) Near stream superficial flow paths. (b) and (c) Lateral subsurface flow (c is initiated only after a groundwater raise upslope). The TTD model (blue pdf) is a simplification of reality that works well for simulating (blue curve) a given tracer output measured in a discrete manner (red dots). Adapted from Rodriguez and Klaus (2019)

(McGuire & McDonnell, 2006; Stewart, Morgenstern, & McDonnell, 2010), where the tracers used to infer them are sampled at lower frequencies (mostly weekly to monthly). However, only strong assumptions about the system boundary conditions and its internal transport mechanisms (Leray et al., 2016; Małoszewski & Zuber, 1982) can lead to such unimodal distributions. Multimodal and irregular shapes of TTDs are instead found with physically based transport models, even in steady-state conditions (Engdahl & Maxwell, 2014; Goderniaux, Davy, Bresciani, de Dreuzy, & Le Borgne, 2013).

A number of studies advocated the use of multimodal TTDs in the context of steady-state (Leray et al., 2016, p. 78, and citations below). At different scales, contrasts in water velocities or in flow path lengths may generate multimodal TTDs. Contrasting flow path lengths can for example come from: stream channel morphological features (Haggerty, Wondzell, & Johnson, 2002; Ward, Schmadel, & Wondzell, 2018), competing recharge areas to a groundwater well (Cirpka et al., 2007; Massoudieh, Sharifi, & Solomon, 2012; Visser, Broers, Purtschert, Sültenfuß, & de Jonge, 2013), different sources of surface water or groundwater (Duy et al., 2019; Stolp et al., 2010) or shallow and local vs. deep and regional subsurface flows (Goderniaux et al., 2013; Solomon, Genereux, Plummer, & Busenberg, 2010; Wilusz, Harman, Ball, Maxwell, & Buda, 2020). Contrasting water velocities can originate from: preferential flow in soil macropores (Jackisch et al., 2017; Klaus, Zehe, Elsner, Külls, & McDonnell, 2013; Scaini et al., 2017; Utermann, Kladivko, & Jury, 1990; White, Dyson, Haigh, Jury, & Sposito, 1986), heterogeneous rock permeability (Desbarats, 1990; Eberts, Böhlke, Kauffman, & Jurgens, 2012; Ritzi et al., 2000; Weissmann, Zhang, LaBolle, & Fogg, 2002) or conduit flow bypassing rock matrix flow in karst geologies (Long & Putnam, 2009).

In unsteady conditions, multiple peaks can be found in TTDs because of dynamic hydrological fluxes (Botter et al., 2010; vander Velde et al., 2012). However, clusters of peaks in the TTD can be related to different major transport processes to an outlet. van der Velde, de Rooij, Rozemeijer, van Geer, & Broers (2010, Figure 6) found time-varying discharge TTDs with two distinct groups of peaks, the first one being intermittent and associated with tile drainage of the root zone storage (younger water) and the second being permanent and associated with slower groundwater flows in the subsurface. Recent numerical experiments on real or virtual hydrological systems (Danesh-Yazdi, Klaus, Condon, & Maxwell, 2018; Kaandorp, de Louw, van der Velde, & Broers, 2018; Remondi et al., 2018; Yang, Heidbüchel, Musolff, Reinstorf, & Fleckenstein, 2018) showed that, even if SAS functions simplify the shapes of the age distributions compared with TTDs, they may not be described well by unimodal distributions. Rodriguez and Klaus (2019) used high frequency (i.e., sub-daily) stable isotopes in precipitation and discharge over 2 years and found that the SAS function in a slate catchment with complex flow paths may contain several peaks consistent with experimentally identified discharge generation processes.

There is an emerging perception that TTDs in hydrological systems are complex and may be multimodal for reasons other than time-varying hydrological fluxes. However, studies that supported TTD multimodality had only little or no tracer data to constrain model predictions and to validate the simulated TTD shapes. Thus, the existence of high-quality data is crucial to advance our knowledge of TTD shapes. The recent improvements in ^{2}H and ^{18}O measurement techniques (Gupta, Noone, Galewsky, Sweeney, & Vaughn, 2009; Lis, Wassenaar, & Hendry, 2008) and sampling methods (Berman, Gupta, Gabrielli, Garland, & McDonnell, 2009; Herbstritt, Gralher, & Weiler, 2019; Koehler & Wassenaar, 2011; Munksgaard, Wurster, & Bird, 2011; Pangle, Klaus, Berman, Gupta, & McDonnell, 2013) allowed a considerable increase in the tracer record lengths up to several decades (Hrachowitz et al., 2009; IAEA, 2019; IAEA and WMO, 2019; Pfister et al., 2017) and in the resolution of tracer data up to minutes (von Freyberg, Studer, & Kirchner, 2017). This has made the detection of the entire shape of the TTDs more feasible than in the past. High-frequency tracer observations can now constrain the left-hand part of TTDs representing the short (e.g., hours to days) and intermediate (e.g., weeks) transport time scales (Rodriguez & Klaus, 2019), while long records of tracers can constrain the right-hand tail of TTDs associated with long transport time scales (e.g., months to years, Rodriguez, Pfister, Zehe, & Klaus, 2019; Neal et al., 2011). Tracer time series that span several years at high resolution (von Freyberg, Studer, Rinderer, & Kirchner, 2018) will pave the way for the detailed investigation of water flow paths and their influence on TTDs.

3 | SIMULATIONS OF TRACER CONCENTRATIONS THROUGH SAS FUNCTIONS

We focus on the multimodality of the discharge TTD, seen as the TTD of all the water draining to a single outlet like streamflow, as opposed to the TTD of the evapotranspiration flux. Thus, the terminology 'TTD' or 'SAS function' will always refer to discharge unless specified otherwise.

From a mathematical perspective, the TTD is the transfer function that verifies the equation:

$$C_Q(t) = \int_{T=0}^{+\infty} C_J(t-T)\, p_Q(T,t)\, dT \tag{1}$$

where $C_Q(t)$ is the tracer concentration in discharge at time t, $C_J(t - T)$ is the tracer concentration in precipitation at time $t - T$ and $p_Q(T, t)$ is the time-variant TTD, that is, the distribution of water ages T (time spent since entry in the catchment) in discharge conditioned on time t. The same equation applies to outflows other than discharge and their TTDs (e.g., to the evapotranspiration flux ET and its TTD $p_{ET}(T, t)$). Equation 1 is valid only for 'ideal' tracers (such as deuterium or oxygen 18 in certain conditions), for which the concentration associated with a water parcel does not change along its transport. In these circumstances, the TTD assumes the character of a lumped model representing a hypothesis about the transport processes to the outlet.

For non-ideal tracers such as solutes undergoing chemical reactions, the changes in concentration since the tracer entrance into the system need to be accounted for. Assuming that these changes are a direct function of water age T allows using Equation 1 to simulate non-ideal tracers in outflows as well (Maher, 2011; Rinaldo & Marani, 1987). In such a case, $C_J(t - T)$ is replaced by $C_S(T, t)$, i.e., the tracer concentration of water in storage with age T at time t. For atmospheric tracers that are introduced through precipitation and decay with age such as tritium (Stewart et al., 2010; Visser et al., 2019), the following relationship can be implemented: $C_S(T,t) = C_J(t-T)e^{-T/\tau_{dec}}$, where τ_{dec} is a kinetic (decay) constant (e.g., 17.77 years for tritium). For geogenic reactive tracers like silicon and sodium (Benettin et al., 2015; Clymans et al., 2013; Hornberger, Scanlon, & Raffensperger, 2001; Johnson, Likens, Bormann, & Pierce, 1968; Maher, 2010), where the input is typically tracer-free and tracer concentration can increase with age towards some limiting concentration C_{lim}, the storage concentration takes the form: $C_S(T,t) = (C_J(t-T) - C_{lim})e^{-T/\tau_{eq}} + C_{lim}$, where τ_{eq} is a kinetic constant (e.g., 1 year). Tracer concentrations in storage can also increase because of specific removal of tracer-free water by ET (evapoconcentration). The resulting effect on $C_S(T, t)$ is explained in detail by Queloz, Carraro, et al. (2015) and can be formulated through an evapoconcentration parameter α, where α = 0 represents pure evapoconcentration and α = 1 represents fully conservative tracer behaviour (Bertuzzo, Thomet, Botter, & Rinaldo, 2013).

The unsteady TTDs $p_Q(T, t)$ can be obtained by solving a water balance equation for each water parcel [usually referred to as age master equation (Botter et al., 2011)]. Numerical solutions to the age master equation (Benettin & Bertuzzo, 2018; Harman, 2015; Rodriguez & Klaus, 2019; vander Velde et al., 2012; Visser et al., 2019) usually consider one control volume for the entire hydrological system and use the 'age-ranked storage' $S_T(T, t)$ as state variable. S_T represents the distribution of water volumes in storage, ranked by age. For instance, S_T = 10 mm for T = 1 day means that 10 mm of water in storage is younger than 1 day. S_T changes with time because new water is introduced by precipitation J, and because ages in storage are removed by outflows Q and ET. These outflows are associated with SAS functions Ω_Q and Ω_{ET} representing their preference for removing certain ages in storage. Time-varying TTDs are obtained by evaluating the SAS functions over the age-ranked storage:

$$p_Q(T,t) = \frac{\partial}{\partial T}(\Omega_Q(S_T,t)) \tag{2}$$

In some circumstances, it may be convenient to consider the normalised form of the ranked storage $P_S = S_T/S(t)$ and use SAS functions $\Omega_Q(P_S, t)$ that are defined over the interval [0,1], where 0 corresponds to the youngest parcel in storage and 1 to the oldest. In this work we also refer to the SAS functions in non-cumulative form, simply defined as $\omega_Q(S_T, t) = \partial\Omega_Q/\partial S_T$ or $\omega_Q(P_S, t) = \partial\Omega_Q/\partial P_S$. Tracer concentrations are obtained by coupling Equations 2 to 1 after imposing a functional form to the SAS functions. Examples of SAS function shapes are the power function (Benettin, Soulsby, et al., 2017), the beta distribution (van der Velde et al., 2015), the gamma distribution (Harman, 2015), or any of the functions described in section S1. Here, we test composite SAS functions obtained as a weighted sum of probability distributions:

$$\begin{cases} \Omega_Q(y,t) = \sum_{m=1}^{M} \lambda_m(t)\Omega_m(y,t) \\ y = S_T \text{ or } y = P_S \end{cases} \tag{3}$$

The M functions $\lambda_m(t)$ are time-varying weights summing to 1 to ensure mass conservation. In this study, we used constant weights, but they can be parameterised to change with various hydrological quantities such as precipitation intensities, storage, or storage variations (Rodriguez & Klaus, 2019). Each weight $\lambda_m(t)$ defines the relative volumetric contribution of the component $\Omega_m(y, t)$ to the considered outflow [here discharge $Q(t)$] at time t. $\Omega_m(y, t)$ is a probability distribution function of the variable $y = P_S$ or $y = S_T$ associated with a contribution (labelled with m) of water ages to the outflow. This contribution can be a given hydrological process (Wilusz et al., 2020) or a spatial end-member (e.g., soil water) having a particular age range (e.g., young water for overland flow). In this study, we assumed that the $\Omega_m(y, t)$ do not explicitly depend on t. They can nevertheless be explicitly dependent on time t to include the effect of a time-varying age selection for each component and to increase the overall temporal variability of the SAS function (Wilusz et al., 2020). Note that even a SAS function with no explicit dependence on t allows simulations of time-varying TTDs. This differs from previous similar formulations of composite TTDs that were at steady state (Leray et al., 2016). Composite SAS functions can be defined the same way in non-cumulative form. To test our results for a larger number of SAS shapes, we used SAS functions defined both over the age-ranked storage (Section 5) and over its normalised form (Section 4).

4 | MULTIMODALITY IN A LYSIMETER-SCALE EXPERIMENT

Small-scale (~2 m) experimental setups like lysimeters (Pütz et al., 2016) are currently the only hydrological system where TTDs can be measured by labelling individual precipitation events. While tracer experiments in lysimeters often resulted in substantial single-mode tracer breakthrough curves (BTC) (Groh et al., 2018; Stumpp, Nützmann, Maciejewski, & Maloszewski, 2009), the experiment by Queloz et al. (2015) is one rare example showing a clear bimodal behaviour with two distinct peaks in the BTC.

4.1 | Data and methods

Extensive information about the experiment including hydrological and tracer data can be found in Queloz, Bertuzzo, et al. (2015). In brief, the experiment was carried out at EPFL campus (CH) between

2013 and 2014 in a large (2.5 m-depth, 1.2 m^2-diameter) vegetated lysimeter. The experiment was forced by controlled, non-stationary irrigation. Two small willow trees planted within the lysimeter triggered intense evapotranspiration fluxes that regularly exceeded 30 mm/day during warm summer days. Flow from the bottom drainage was discontinuous, with peaks following irrigation and no flow during dry days (Figure 2). A number of five fluorobenzoate (FBA) tracers were applied in Spring 2013 and showed different recoveries. We focus here on the tracer that had the most conservative behaviour (2,6-DFBA, 60% recovery). The tracer arrived at the bottom of the lysimeter over two distinct timescales that resulted in two different major peaks with duration of weeks to months (Figure 2). It is worth to recall here that the TTD is the normalised mass breakthrough curve (MBTC) and not the concentration breakthrough curve (CBTC). The MBTC is influenced by the variability of the hydrological fluxes and would resemble the drainage time series, with multiple individual peaks corresponding to high flow events. Yet, the CBTC better reveals the two longer-lasting peaks and we consider those as representative of contrasting transport processes occurring within the lysimeter. The major of the two peaks occurred through the summer (roughly 3 months after application) when flow was very discontinuous, while the other peak occurred at the beginning of the winter (roughly 6 months after application), when evapotranspiration became significantly lower. Although the second peak is smaller in magnitude compared with the first peak, it drained more tracer mass because flows were higher.

Tracer transport for this experiment was previously modelled by (Queloz, Carraro, et al., 2015), who used an approach based on SAS functions and conceptualised the lysimeter as two systems in series: the unsaturated soil (modelled through a power-function SAS) and the saturated gravel filter (modelled as a fully mixed compartment). In this study, we use one single control volume for the entire lysimeter system (unsaturated and saturated) and we test a new functional shape for the SAS function $\Omega_Q(P_S)$. We introduce the truncated normal SAS function $\mathcal{N}_T(P_S,m,s)$ (formula in S1.1), which has two parameters: m, corresponding to the mode of the distribution and s, which is proportional to the standard deviation of the distribution. Depending on the value of the parameters, the normal SAS function can be bell-shaped or not. Note that even a symmetric SAS function does not imply that the resulting TTDs are symmetric. As the parameters of the normal SAS function are strongly related to the function mode, it is an appealing candidate to explore multimodality. Thus, we generated a composite SAS function as the linear combination of two normal SAS functions (see section S1.1). The composite function allows for two distinct peaks and has a total of five calibration parameters (two for each normal distribution and one for the partitioning). For comparison, we also used a single normally distributed SAS function (two parameters) and a power-function (one parameter) for Ω_Q. The SAS function for the ET flux (Ω_{ET}) is assumed in all cases to be a uniform distribution over the younger storage fraction defined by the parameter u, as proposed by Harman (2015). The model further assumes that the tracer is conservative but only partially taken up by vegetation, through a parameter $\alpha \leq 1$ (see Section 3). This partial uptake of the FBA tracer by the willow trees in the lysimeter was revealed by Queloz, Bertuzzo, et al. (2015) who found small amounts of tracer in plant tissues, and whose breakthrough curves were not described well either by an absence of vegetation uptake, or by a complete vegetation uptake of the tracer. The simulation was run using *tran*-SAS (Benettin & Bertuzzo, 2018) and calibrated to measured tracer data through the $DREAM_{ZS}$ algorithm (ter Braak & Vrugt, 2008; Vrugt et al., 2009). Calibration was based on the assumption that residuals were independent and normally distributed. Further details on the model and calibration setup can be found in Section S2. For each of the three tested SAS models, the best parameter combination (Table S1) was retained to obtain the instantaneous TTDs and compute the marginal TTD.

4.2 | Results

The results of the tracer breakthrough simulations are shown in Figure 3 together with their corresponding SAS function Ω_Q. Breakthrough curves are discontinuous because of the frequent absence of flow during the dry summer months. The three curves all match the beginning of the early breakthrough in mid-May 2013. This 1-month delay since tracer application is obtained through SAS functions that, in all cases (see Figure 3 inset), are almost null up to P_S = 0.2, meaning

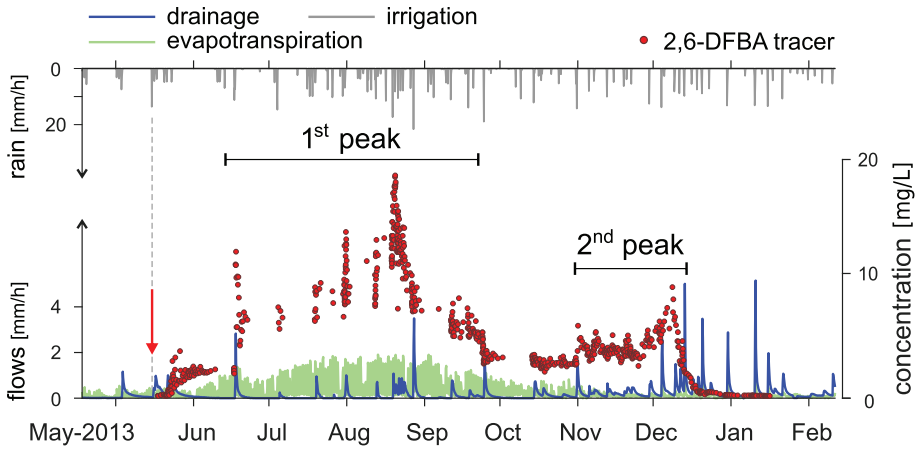

FIGURE 2 Experimental data from the lysimeter experiment by Queloz, Bertuzzo, et al. (2015). The vertical arrow marks the tracer application in mid May 2013. Tracer measurements highlight the occurrence of two major peaks in the tracer breakthrough: the first one occurred through the summer when flow was very discontinuous; the second occurred at the beginning of the winter when evapotranspiration became considerably lower

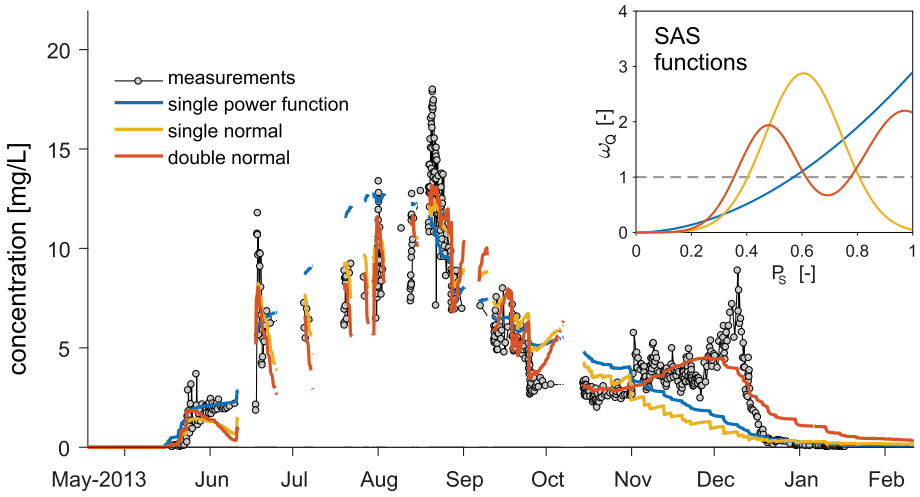

FIGURE 3 Tracer concentration in the lysimeter drainage as simulated by the calibrated models. Curves are discontinuous during periods with no flow. The inset reports the calibrated StorAge Selection function for each model

that drainage does not comprise the 20% younger soil waters. The three simulations are also fairly similar at reproducing the first wide peak from June to October, with the power-function simulation less-variable and slightly higher than the tracer peak, but overall broadly comparable with measurements. The main difference occurs upon the second peak, which is entirely missed by the simpler models while it is captured by the double normal SAS function. The higher accuracy obviously comes at a cost (five SAS parameters instead of 1 or 2) but, besides a much better performance (see additional analyses in Section S2), the double normal model is more appropriate because it allows expressing the multimodality of the data. As a result, model errors are symmetric and much less correlated than in the other cases (Figure S2 and Table S2). The marginal TTDs resulting from the three models are illustrated in Figure 4. As expected, the marginal TTD resulting from the multimodal SAS function has two distinct peaks: the first at 90–100 days and the second at 200–250 days. By contrast, the marginal TTDs resulting from other SAS functions have a single and higher peak at 90–100 days and underestimate the older water contribution in the right tail of the distribution. These simulations ultimately tell us that in all cases, water found at the bottom drainage is representative of the older water stored in the lysimeter (Figure 3, inset). However, two major transport mechanisms emerge from the data and the simulations: some water is relatively fast and it is able to percolate during the dry summer season (c.f. first peak of the CBTC), likely due to the occasional activation of preferential pathways; the rest of the tracer mass moves with the matrix flow and takes more than twice as much to reach the lysimeter bottom (c.f. second peak of the CBTC).

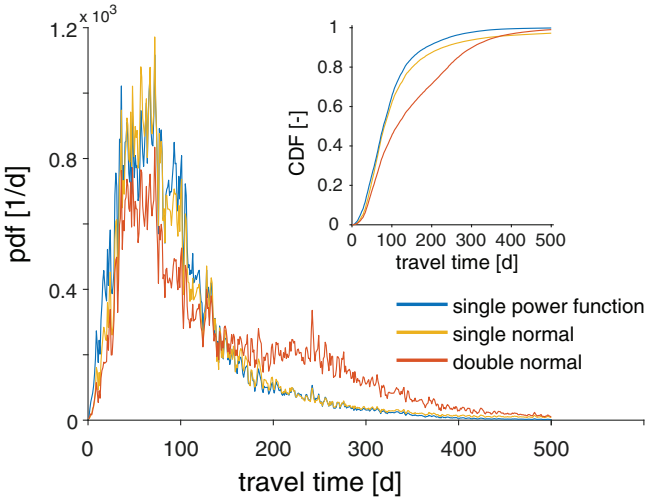

FIGURE 4 Marginal travel time pdf (main figure) and CDF (inset) computed from the calibrated models

5 | MULTIMODALITY IN A VIRTUAL, CATCHMENT-SCALE EXPERIMENT

The tracer breakthrough experiment shown in Section 4 cannot be easily applied at larger scales (e.g., hillslopes, catchments). Thus, the applicability of these results and the validity of these conclusions at larger scales require a numerical experiment.

5.1 | Methods

We consider a virtual catchment with an arbitrary scale, with known fluxes J, ET, Q, and with known deuterium content in precipitation C_J. These fluxes and tracer concentration have a yearly seasonality and have random daily variations (supplementary information SI, section S3). The true transport processes to the stream are summarised by a constant, bimodal composite SAS function $\Omega^{ref}(S_T)$ ($\omega^{ref}(S_T)$ in non-cumulative form), made of a sum of two gamma distributions Ω_1 and Ω_2 (or ω_1 and ω_2) corresponding to a young water component and an old water component (Equation S6). Here, age-ranked storage S_T is employed to allow the use of gamma distributions. To reduce the number of variables, we used a uniform distribution (random sampling of all ages) for the SAS function of ET (Ω_{ET}). The 'observed' deuterium composition of discharge is generated according to Equations 1 and 2 using the multimodal Ω^{ref} as SAS

function. We tested the ability of a simpler, unimodal SAS function Ω_Q (one constant gamma distribution, Equation S5) to simulate the observed stream δ^2H. The two parameters of Ω_Q were calibrated against observed stream δ^2H using a Monte Carlo procedure and the Nash-Sutcliffe Efficiency to evaluate model performance (SI, section S3). We additionally simulated three other solutes with $\Omega^{ref}(S_T)$ and compared these 'observations' to the simulations obtained from the unimodal SAS function Ω_Q calibrated to δ^2H. This was done to assess the performance of the unimodal approximation of the SAS function for water quality simulations. We considered:

- A virtual pesticide (e.g., Atrazine) with a short kinetic (decay) constant τ_{dec} = 50 days (<0.5 MTT, Table 1), applied as a single pulse C_0 = 50 mg/L during a 100 mm precipitation event over 1 day.
- Nitrate (NO_3^-), with a long-term input of 60 mg/L, then linearly decreasing from 60 mg/L to 0 in 150 days (≃0.5 MTT, Table 1).
- A weathering product (e.g., silicon) with a long kinetic constant τ_{eq} = 550 days (≃2 MTT, Table 1) and limit concentration C_{lim} = 200 mg/L.

The additional tracer concentrations were obtained from the following equation (similar to Equation 1):

$$C_Q(t) = \int_{T=0}^{+\infty} C_S(T,t) p_Q(T,t) dT \quad (4)$$

where $C_S(T, t)$ has a different expression depending on the considered solute (Section 3, and SI, section S3). These additional tracers have Damköhler numbers between roughly 0.5 and 6 for the considered catchment (ratio of MTT to kinetic constant, see Oldham, Farrow, & Peiffer, 2013; Maher & Chamberlain, 2014; Ameli et al., 2017), representing from reaction-limited to transport-limited tracer dynamics, respectively. The pesticide, with a low Damköhler number, will thus be highly sensitive to the accuracy of the model in rapidly transporting water to the outlet. Conversely, the weathering product, with a high Damköhler number, will be highly sensitive to the accuracy of the model in retaining water for a long time in storage until it nearly reaches chemical equilibrium.

5.2 | Results

The unimodal gamma-distributed Ω_Q simulated the observed stream δ^2H well, with a Nash-Sutcliffe Efficiency of NSE = 0.89 (Figure 5a). The model only failed to reproduce some of the rapid δ^2H responses, especially at the beginning of wetter periods. The corresponding calibrated Ω_Q is similar to the old water component Ω_2 of the SAS function Ω^{ref} (Figure 5). As such, it clearly neglects the young water component Ω_1 ($S_T \lesssim 200$ mm), and it overestimates the old water fractions ($S_T \gtrsim 600$ mm) compared with Ω_2. This is also visible in the corresponding marginal TTDs (average TTD over 100 years) (Figure 6), which have the largest differences over both younger ($T \lesssim 0.2$ year) and older ($T \gtrsim 1$ year) water components. The observed differences between Ω^{ref} and Ω_Q did not have a large influence on the simulations of the stream δ^2H. To assess the consequences of those differences for other tracers, we compared the simulations from those two models for the three additional solutes in the stream. The observed differences between the unimodal Ω_Q calibrated to δ^2H and the bimodal Ω^{ref} are well reflected in the simulations of these three tracers. Because of the mismatch in old water fractions ($T \gtrsim 1$ year, Figure 6), Ω_Q constantly overestimates the concentration in weathering product (Figure 5b). The mismatch in intermediate ages ($0.25 \lesssim T \lesssim 1$ year) results in a slower middle-term response of Ω_Q to a change in the nitrate input (Figure 5c), with a 6 months delay to return to concentrations below the WHO guideline of 50 mg/L and about 2 years more to return to nitrate-free water. Finally, without a young water component ($T \lesssim 0.2$ years), the unimodal Ω_Q does not simulate the quick pesticide breakthrough (Figure 5d) nor does it simulate a long-term response because of the quick decay of the pesticide (τ_{dec} = 50 days). The differences in water age between the two models are quantified through some statistics of the marginal age distributions (Table 1). The unimodal Ω_Q results in a much larger mean travel time (MTT) (explaining the delay in middle-term response in nitrate), in a fraction of water younger than τ_{dec} 58 times lower, and in a higher fraction (13% more) of water older than τ_{eq}.

TABLE 1 Statistics of the marginal travel time distributions arising from the unimodal (Ω_Q calibrated to δ^2H) and multimodal ('true' Ω^{ref}) StorAge Selection functions

	Ω^{ref} (true multimodal gamma)	Ω_Q (calibrated unimodal gamma)
MTT [years]	0.81	1.22
MdTT [years]	0.72	0.94
$F(T < 2$ days) [%]	0.049	0.00
$F(T < 7$ days) [%]	0.47	0.00
$F(T < 31$ days) [%]	6.5	0.023
$F(T < \tau_{dec} = 50$ days) [%]	8.7	0.15
$F_{yw}(T < 73$ days) [%]	10	0.82
$F(T < 2\ \tau_{dec} = 100$ days) [%]	13	2.5
$F(T < 3\ \tau_{dec} = 150$ days) [%]	20	8.7
$F(T < 365$ days) [%]	73	55
$F(T < \tau_{eq} = 550$ days) [%]	90	77
$F(T < 2\ \tau_{eq} = 1{,}100$ days) [%]	99	95
$F(T < 3{,}000$ days) [%]	≃ 100	99.7

Abbreviations: MdTT, median travel time; MTT, mean travel time.

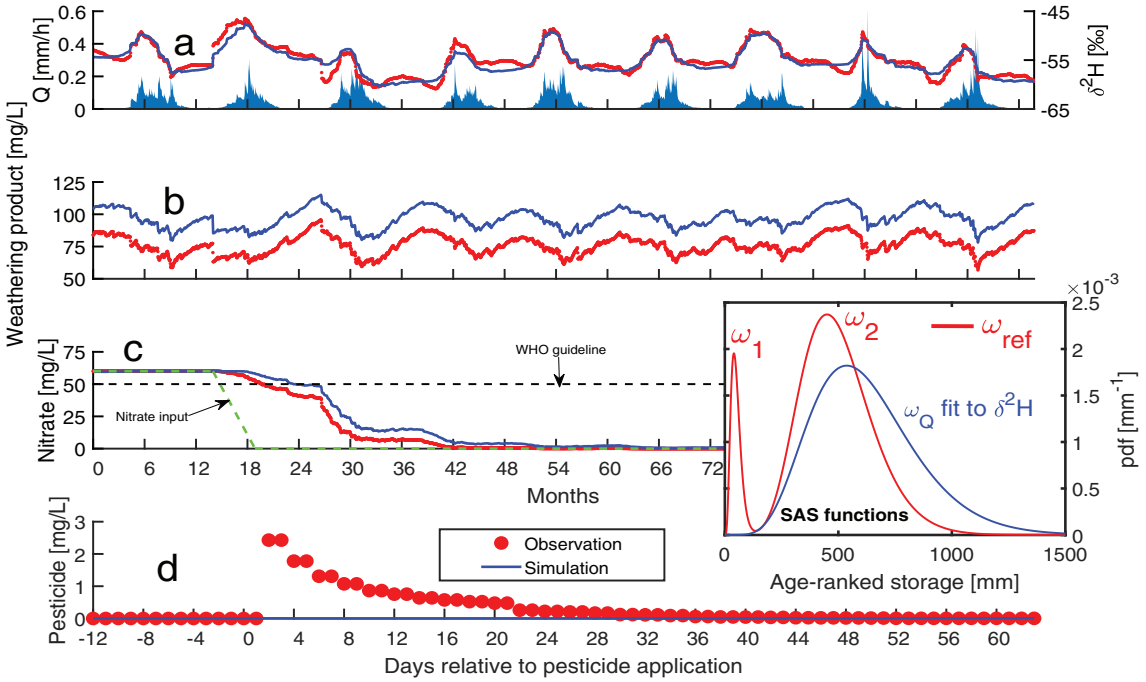

FIGURE 5 Simulations (blue curves) and observations (red dots) of tracers in the stream of the virtual catchment. The 'observations' correspond to the tracer values obtained using the reference bimodal StorAge Selection function Ω_{ref} (or ω_{ref} in non-cumulative form, weighted sum of components ω_1 and ω_2), while the 'simulations' correspond to tracer values obtained using the best fit of a gamma distributed Ω_Q (or ω_Q in non-cumulative form) to 'observed' δ^2H. (a) Simulation calibrated to the observed δ^2H (NSE = 0.89), (b) associated concentrations in weathering product (C_{lim} = 200 mg/L, τ_{eq} = 550 day), (c) associated NO_3^- concentrations, and (d) associated pesticide concentrations (τ_{dec} = 50 day). The nitrate input decreases linearly from 60 to 0 mg/L in 150 days. The dashed line in (c) indicates the WHO guideline of 50 mg/L as NO_3^-. The pesticide instantaneous input occurs at day 2 as 100 mm of precipitation at 50 mg/L

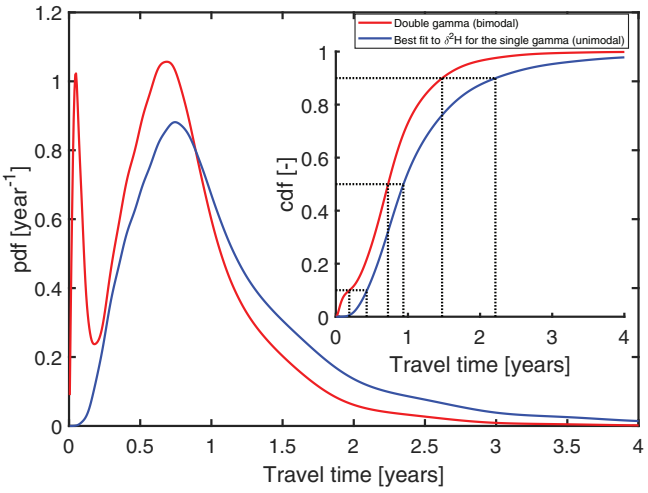

FIGURE 6 Marginal (averaged over 100 years) travel time pdf (main figure) and CDF (inset) for the virtual catchment computed from the 'true' bimodal Ω_{ref} (red) and from the unimodal gamma Ω_Q calibrated to stream δ^2H (blue)

These results show that, despite the ability to simulate the observed δ^2H, the calibrated unimodal Ω_Q fails to simulate other tracers. Overall, we can expect that a deviation of a model (here Ω_Q) from the 'truth' (usually unknown, but here Ω^{ref}) around a given age T will create a mismatch for all tracers whose stored concentrations vary with a time scale close to T. For instance, the unimodal approximation is reliable only for travel times close to 1 year (Figure 6, the curves cross around T = 1 year). δ^2H in storage depends on the δ^2H of precipitation, which essentially varies over a whole year. Thus, the unimodal approximation matches the time scale of δ^2H dynamics, and the simulations of δ^2H in the stream are accurate. For all the other solutes, the large differences between the unimodal approximation and the true age description exactly correspond to the time scales of the tracer dynamics in storage, and the simulations are wrong.

6 | DISCUSSION

6.1 | Relevance of water age multimodality for tracers

Our results confirm the ability of age-based lumped models to simulate tracer dynamics in discharge. Unimodal SAS functions only had one or two parameters but they provided satisfactory simulations with good performance measures. This is because they managed to capture the average tracer dynamics (e.g., as seen through a moving average) resulting from the range of travel times that characterises the majority of the discharge. For the lysimeter, 50% of the water left via the bottom drainage in less than 100 days, which is captured by the power function and the single normal function well enough

(Figure 4). For the virtual catchment, 50% of the water left via discharge in less than 1 year, which is captured by the single gamma distribution well enough (Figure 6). Detailed characteristics of the tracer observations such as flashy responses associated with small discharge volumes (e.g., short-term dynamics within each peak in Figure 3, months 24–30, 12–16, and 52–56 in Figure 5), or secondary peaks (Oct–Jan in Figure 3) do not need to be reproduced to obtain satisfactory values of the standard objective functions used for calibration. Yet, these detailed characteristics represent transport processes acting at different time scales and they can be highly informative on the deficiencies of a too simple model. They could also be used as 'soft data' (Seibert & McDonnell, 2002) along with experimental knowledge to justify the selection of more complex age models accounting for more hydrological processes (as in Rodriguez & Klaus, 2019).

Composite SAS functions increased model complexity but in return gave more accurate process representation. For instance, the double normal model applied to the lysimeter experiment (Section 4) was able to capture the two main timescales at which the tracer was transported through the lysimeter, while the simpler models underestimated the impact of longer transit times (Figures 3 and 4). In some cases, the increase in performance could be insufficient to justify the use of additional parameters. For example, for the catchment-scale virtual experiment, the performance in δ^2H of the single gamma model does not motivate the use of a more complex model. This highlights that a single tracer measured in inflows and outflows may not allow the identification of all peaks of the TTDs. Furthermore, the virtual catchment experiment showed that the simpler model, although efficient enough in reproducing δ^2H, essentially failed to simulate the three other tracers. The unimodal approximation neglected the short term response of the catchment, it delayed the middle term response, and it overestimated the long-term response. This shows that simulations of solute chemistry require an accurate estimation of the TTDs that goes beyond conservative tracer input–output relationships, and that accounts for the potential multiple modes of transport associated with different age fractions (Benettin et al., 2017). On the other hand, this also means that stream chemistry data (Neal et al., 2013) and new available tracers (Abbott et al., 2016; Hissler, Stille, Guignard, Iffly, & Pfister, 2014; Pfister et al., 2017; Visser et al., 2019) can be used to validate TTDs deduced from a conservative tracer input–output relationship (Guillet et al., 2019). Overall, these results highlight the need for new methods that do not calibrate TTDs using tracer input–output relationships but instead measure the TTDs directly, such as (Kim et al., 2016; Kirchner, 2019).

Several characteristics shared by the two hydrological systems described in Sections 4 and 5 made the comparison between unimodal and multimodal models possible. Contrary to previous studies on the shape of TTDs and SAS functions, our work was not impacted by large unknowns such as total storage (Birkel, Soulsby, & Tetzlaff, 2011; Rodriguez, McGuire, & Klaus, 2018) and unknown past inputs and initial conditions (Hrachowitz, Soulsby, Tetzlaff, & Malcolm, 2011). In addition, there was no uncertainty related to hydrological and tracer data regarding the spatial homogeneity of inputs, the calculations of ET, the limited tracer sampling frequency (Hrachowitz et al., 2011; Kirchner, Feng, Neal, & Robson, 2004; Stockinger et al., 2016) and record length (McGuire & McDonnell, 2006). In addition, we avoided using several common modelling assumptions that may have a noticeable impact on the inferred age distributions. These assumptions include the no-flow boundaries defining the control volume to ensure the closure of the mass balance (related to the calculation of actual ET and/or deep water losses), and the ages of water used by ET. van der Velde et al. (2015) and Ali, Fiori, and Russo (2014) showed that the ET flux and its TTD influence the TTD of discharge. Further research is needed to improve our understanding of the role of the water ages abstracted by *ET* on the shapes of the discharge TTD (via the effect of Ω_{ET} on S_T or P_S hence p_Q).

6.2 | Interpretations of the water age uni- or multimodality

To understand the possible reasons for the multimodal character of TTDs not simply caused by time-varying inflows and outflows, it may useful to see the travel time T of an individual water parcel from a Lagrangian point of view (i.e., following the water parcel on its journey). The travel time can be expressed as $T = L/v$, where L is the total length of the flow path taken by that particle (from entry into the system to exit), and v is the harmonic mean of Lagrangian velocities of that parcel along the considered flow path of length L (see SI, section S4). The harmonic mean of velocities is used to obtain an average that appropriately summarises the entire history of Lagrangian velocities along the flow path in a single measure. We use this particular point of view as a simplification that helps us focusing on the role of flow path lengths and velocities in shaping the TTD, whereas potentially more complex Lagrangian representations of water transport are possible (Berkowitz, Cortis, Dentz, & Scher, 2006; Botter, Bertuzzo, Bellin, & Rinaldo, 2005; Cvetkovic, Carstens, Selroos, & Destouni, 2012; Davies, Beven, Rodhe, Nyberg, & Bishop, 2013; Sternagel, Loritz, Wilcke, & Zehe, 2019; Zehe & Jackisch, 2016). Using a similar approach, Kirchner, Feng, and Neal (2001) calculated the shape of TTDs for theoretical catchment geometries corresponding to various distributions of L [called width function $w(x)$, with x the distance to the stream]. Seeing both L and v as random variables makes the TTD a ratio distribution (Rinaldo, Vodel, Rigon, & Rodriguez-Iturbe, 1995). Ratio distributions generally do not have simple analytical expressions (Curtiss, 1941), meaning that the shape of the TTDs can be complex, with potentially many peaks and often a heavy tail. In particular, if the distributions of L and v are multimodal for various physical reasons (see Section 2), it can be expected that the TTD is multimodal as well (see Figure 7, note, however, the implicit assumption of independence between L and v). This has been recently observed in a catchment in Switzerland where the extension and the contraction of the flow network for different wetness conditions creates complex patterns of flow paths leading to multimodal TTDs (assuming a constant, homogeneous velocity field) (van Meerveld, Kirchner, Vis, Assendelft, & Seibert, 2019). In reality, the shape of

TTDs will depend on the relationship between L and v. In catchments, it can be expected that the location of a given input will determine L, but also v. For instance, in heterogeneous media, dispersion causes the distribution of v to broaden and flatten with increasing L (Le Borgne, de Dreuzy, Davy, & Bour, 2007). This can be interpreted as an increased probability with time that the advective velocity of a water particle has changed along its transport (e.g., as in Davies et al., 2013; Scaini, Amvrosiadi, Hissler, Pfister, & Beven, 2019; Zehe & Jackisch, 2016). Therefore, L and v are probably not independent, making the TTD, as the pdf of their ratio, difficult to estimate a priori (Curtiss, 1941). Consequently, even a complete knowledge of the distributions of L and v may not allow to determine the TTD as it was done in Figure 7 by assuming that L and v are independent.

At large scales (e.g., hillslope, catchment), L can be much larger than the scale of the heterogeneous properties of the porous media (i.e., different pore sizes, macropore network, rocks, roots, etc.). As a result, dispersion is strong and the differences in travel time T between the water particles coming from different parts of the catchment (with different L) can be attenuated. This may explain the general validity of unimodal TTDs in catchments (McGuire & McDonnell, 2006). For instance, Kirchner et al. (2001) found that low Péclet numbers (i.e., advection $\ll$ dispersion) are needed to explain the gamma shape of TTDs suggested by the spectral slopes of stream chemistry. At smaller scales, L can be small compared with the scale of heterogeneities (i.e., advection $\gg$ dispersion) such that the TTDs are more likely to be multimodal. For example, preferential flow in soils can cause a strongly bimodal distribution for v. In the lysimeter at EPFL (Section 4), flow paths are mostly vertical and the transport distance is probably narrowly distributed around L = 2.5 m (the depth of the soil column). The multimodal TTDs obtained in the lysimeter are thus due to contrasting velocities coming from preferential flow vs. matrix flow in the lysimeter (Figure 7a), which was clearly identified from comparisons of tracers measured in soil water vs. discharge (Benettin, Queloz, Bensimon, McDonnell, & Rinaldo, 2019). The importance of preferential flow in soils for catchment-scale TTDs may be difficult to evaluate. Glaser, Jackisch, Hopp, and Klaus (2019) showed in the Weierbach catchment (Luxembourg) that rainfall-runoff simulations were not improved by modelling vertical preferential flow at the catchment scale, using the soil preferential flow parameters deduced from plot-scale tracer breakthrough experiments. However, non-uniform lateral flow (similar to lateral preferential flow) appeared to be an important mechanism for discharge generation in this

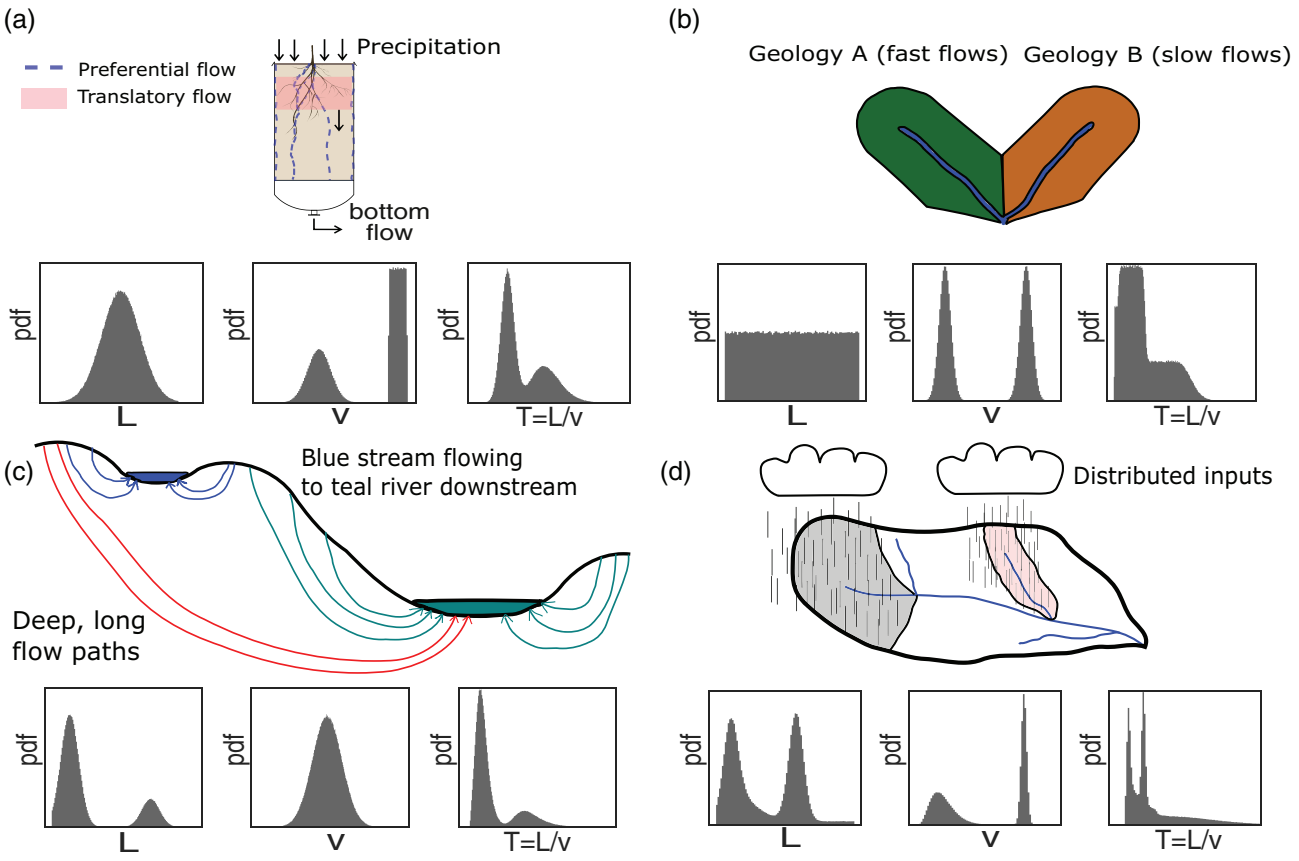

FIGURE 7 Four cases where multimodal TTDs are expected: preferential flow vs. translatory flow in soils (c.f. lysimeter at EPFL) (a), different geologies leading to contrasting water velocities in subcatchments with similar geometry (b), shallow, local vs. deep groundwater contributions to a river draining several subcatchments (c), and distributed precipitation over a large catchment with different geological units and different subcatchment geometries (d). Expected distributions of flow path length L and average water velocity v (harmonic mean), and the multimodal distribution of travel times T calculated as the pdf of L/v are shown

catchment, and it could be implemented in the model by using a highly conductive horizontal soil layer (Glaser et al., 2019). Different conclusions regarding preferential flow were found by van Schaik et al. (2014), who highlighted its non-negligible role for runoff simulations during extreme rainfall events in a semi-arid catchment in Spain. This suggests that preferential flow has an influence on a catchment TTD only if it provides sufficient volumes of water to the outlet.

Our results suggest that different hydrological processes generate multimodal TTDs only if these processes result in contrasting water ages and provide comparable volumes of water. For instance, if surface runoff reaches the stream in 1 hour, there may be no detectable peak in the TTD around T = 1 hour if 99% of discharge is generated by subsurface stormflow having water of at least 1 week of age. Similarly, if two recharge areas to a groundwater well provide similar water ages, the TTD of the well will be unimodal regardless of the sizes of each recharging area. Composite SAS functions provide an intuitive mathematical representation: multiple peaks are observed in the marginal TTDs if the different probability distribution functions summed together in the SAS function are far from each other in the age domain (T, P_S, or S_T), and if they are associated with weights λ (Equations S3 and S6) that are comparable (e.g., 25% and 75%).

6.3 | Process knowledge and the shape of composite SAS functions

The characteristics (number of peaks, peak amplitudes, and age ranges) of multimodal age distributions can be deduced from experimental knowledge of hydrological processes and are useful to test hypotheses about these processes (Rodriguez & Klaus, 2019). In this case, a step-wise increase in the complexity of the age distributions may allow a better understanding of the complexity of the hydrological system enciphered in the tracer data. For instance, one may start with an age component for young water after detecting surface runoff in the catchment and mapping its extent from manual survey and/or aerial images. The characteristics of this age component may then be deduced from GIS analysis, using initially simple assumptions of flow paths and water velocities (c.f., van Meerveld et al., 2019). Spectral slopes of stream chemistry suggest that a gamma distribution with a shape parameter $k < 1$ may be an appropriate candidate for this young water component (Kirchner et al., 2000). However, a uniform distribution on a small age range may perform well for tracer simulations, and may avoid numerical issues due to the asymptote at age 0 of the gamma distribution with $k < 1$ (Rodriguez & Klaus, 2019). Older water components may then be deduced from estimates of soil water storage and age (based for instance on soil moisture measurements, hydraulic turnover time) and hydrogeological knowledge of the aquifer (no-flow boundaries, hydraulic conductivity, groundwater depth) for the groundwater component. The functional form of older components may be chosen among popular functions, such as the power function (Benettin, Soulsby, et al., 2017; Queloz, Carraro, et al., 2015) or the beta distribution (Danesh-Yazdi, Botter, & Foufoula-Georgiou,-2017; Kaandorp et al., 2018; van der Velde et al., 2015; Yang et al., 2018) to use P_S as a variable. The uniform distribution or the gamma distribution (Harman, 2015; Rodriguez & Klaus, 2019; Smith, Tetzlaff, & Soulsby, 2018) may be chosen to use S_T instead, which may reduce the uncertainties related to the usually unknown total storage.

On the other hand, composite SAS functions may more easily lead to over-parameterization and the related parameter uncertainties (hence age uncertainties) compared with simpler models. In some cases, it may not be possible to conclude that age multimodality exists in the investigated hydrological system (even if it is true) because the available data does not justify the use of more complex models (c.f., for the virtual catchment when considering only δ^2H). This may happen in particular when the employed tracer data is at insufficient resolution or when its record length is too short to reveal the influence of contrasting water age contributions to the outlet. Furthermore, lumped models based on water ages often do not allow identifying hydrological processes on their own due to the 'compression' of information about the hydrological system. This compression is the consequence of the current inability of mathematical models to perfectly reflect all the perceptual information contained in process knowledge. A given composite TTD or SAS function can correspond to many configurations of processes (c.f., Figure 7a,c). This means that the details on the various hydrological processes aggregating to catchment response cannot be derived from water ages alone. Only precise knowledge of potential water flow paths or velocities (such as for the EPFL lysimeter or Biosphere 2 hillslope) may allow such inductive reasoning. Alternatively, such inferences may be possible by linking parts of the TTDs or SAS functions (e.g., components and age ranges) inferred from one tracer to different end-members and spatial contributions identified from other independent tracers. This could be done by sampling more than just catchment inputs (precipitation) and outputs (e.g., streamflow), and by using numerous tracers in End Member Mixing Analysis (Christophersen, Neal, Hooper, Vogt, & Andersen, 1990; Correa et al., 2017; Martinez-Carreras et al., 2015), or by using Bayesian Mixing (Evaristo et al., 2019; Parnell et al., 2013; Zhang, Evaristo, Li, Si, & McDonnell, 2017) when the number of tracers is limited.

6.4 | Modelling complex hydrological systems with complex age distributions

The composite TTDs (Leray et al., 2016) and the composite SAS functions proposed in this study (see also Rodriguez & Klaus, 2019) have the ability to embed a larger variety of processes compared with traditional lumped models, but they are still analytical approximations of potentially more complex distributions. Shape-free distributions are more flexible and could better represent the range of transport processes in hydrological systems. Shape-free distributions can be determined from time series analyses (Turner & Macpherson, 1990), by deconvoluting the tracer output signal (Cirpka et al., 2007; Gooseff et al., 2011; Luo & Cirpka, 2008; McCallum, Engdahl, Ginn, & Cook, 2014), from Bayesian inference using several tracers

(Massoudieh et al., 2012; Massoudieh, Visser, Sharifi, & Broers, 2014), or from multilinear regression analysis (Kirchner, 2019). However, these methods require a large number of tracers (Massoudieh et al., 2014), or tracer time series that are well conditioned for numerical reasons (Kirchner, 2019), and the resulting solutions can be highly non-unique (McCallum et al., 2014). Eventually, analytical solutions can perform better than shape-free solutions in some cases (Massoudieh et al., 2014). Composite TTDs and SAS functions could thus offer a good balance between model parsimony and sufficient representation of the relevant processes at the scale of interest, which is precisely the aim of lumped models.

Spatially explicit models allow a detailed representation of flow paths and transport media properties. These suggest that complex SAS functions and TTD shapes emerge from specific flow paths (Kaandorp et al., 2018; Pangle et al., 2017; Wilusz et al., 2020; Yang et al., 2018) or from various conductivity (or velocity) distributions in the system (Danesh-Yazdi et al., 2018; Davies et al., 2013). Distributed models also allow linking water sources to travel times, providing complementary spatial information that cannot be visualised in lumped models (Sayama & McDonnell, 2009; van Huijgevoort, Tetzlaff, Sutanudjaja, & Soulsby, 2016). However, these models usually require more detailed initial and boundary conditions (Delavau, Stadnyk, & Holmes, 2017; Jing et al., 2019), which get more uncertain at larger scales. In addition, these models are more computationally expensive than their lumped counterparts, and thus require efficient parallelised numerical solutions (Maxwell, Condon, Danesh-Yazdi, & Bearup, 2018). While we often do not have the means to validate the age results from these models, they are useful to explore the possible complexities of the age distributions and relate them to the dominant hydrological processes (Wilusz et al., 2020). This is especially true as these models can much better represent the small-scale mechanisms leading to the observed hydrological processes compared with lumped models, provided that sufficient experimental data is available to characterise well the associated small-scale heterogeneities. In particular, this means that contrary to lumped models, spatially explicit models allow identifying which hydrological processes may lead to complex TTDs and SAS functions.

7 | CONCLUSIONS

Simple TTDs with mainly one peak (or mode) have been prevalent in the last decades because more elaborate models were not needed to obtain a satisfactory tracer simulation. Nevertheless, multimodal TTDs can better describe how different groups of water ages emerge at the outlet of a catchment because of complex flow paths and water velocity distributions. Recent tracer and numerical experiments (including the two examples presented here) show that TTDs with multiple peaks can better simulate the detailed tracer dynamics observed in high-resolution tracer measurements. Moreover, using the TTDs for water chemistry simulations can expose the flaws of a too simple TTD model that underestimates/overestimates large portions of the age distribution with implications for tracer concentrations. Our work highlights that, in various hydrological systems, TTDs are likely to be multimodal because of contrasts in flowpath length or velocity (or both). We provided examples of situations where multimodal TTDs are not simply caused by the dynamics of hydrological fluxes. Multimodality can occur due to: preferential flows in soils, heterogeneity of the catchment geological substratum, deep subsurface flows beyond catchment topographical boundaries, and distributed precipitation over large catchments. Different hydrological processes providing comparable volumes of waters with contrasting ages to an outlet will likely result in multimodal TTDs.

ACKNOWLEDGEMENTS

PB thanks ENAC school at EPFL for financial support. NBR (FNR/CORE/C14/SR/8353440/STORE-AGE) and JK (FNR/CORE/C17/SR/11702136/EFFECT) thank the Luxembourg National Research Fund.

DATA AVAILABILITY STATEMENT

The codes and data used in this study are available on Zenodo (Virtual catchment: http://doi.org/10.5281/zenodo.3686582 and Lysimeter: http://doi.org/10.5281/zenodo.3686596). The mathematical and numerical approaches are very similar to tran-SAS (Benettin & Bertuzzo, 2018). We recommend new users to start with tran-SAS and to define the customized SAS functions they need, following one of the initial SAS function template files.

ORCID

Nicolas B. Rodriguez https://orcid.org/0000-0001-8514-1782
Paolo Benettin https://orcid.org/0000-0001-7556-1417
Julian Klaus https://orcid.org/0000-0002-6301-1634

REFERENCES

Abbott, B. W., Baranov, V., Mendoza-Lera, C., Nikolakopoulou, M., Harjung, A., Kolbe, T., … Pinay, G. (2016). Using multi-tracer inference to move beyond single-catchment ecohydrology. *Earth-Science Reviews*, *160*, 19–42. https://doi.org/10.1016/j.earscirev.2016.06.014

Ali, M., Fiori, A., & Russo, D. (2014). A comparison of travel-time based catchment transport models, with application to numerical experiments. *Journal of Hydrology*, *511*, 605–618. https://doi.org/10.1016/j.jhydrol.2014.02.010

Ameli, A. A., Beven, K., Erlandsson, M., Creed, I. F., McDonnell, J. J., & Bishop, K. (2017). Primary weathering rates, water transit times, and concentration-discharge relations: A theoretical analysis for the critical zone. *Water Resources Research*, *53*(1), 942–960. https://doi.org/10.1002/2016WR019448

Benettin, P., Bailey, S. W., Campbell, J. L., Green, M. B., Rinaldo, A., Likens, G. E., … Botter, G. (2015). Linking water age and solute dynamics in streamflow at the Hubbard brook experimental Forest, NH. *Water Resources Research*, *51*(11), 9256–9272. https://doi.org/10.1002/2015WR017552

Benettin, P., Bailey, S. W., Rinaldo, A., Likens, G. E., McGuire, K. J., & Botter, G. (2017). Young runoff fractions control streamwater age and solute concentration dynamics. *Hydrological Processes*, *31*(16), 2982–2986. https://doi.org/10.1002/hyp.11243

Benettin, P., & Bertuzzo, E. (2018). *Tran*-sas v1.0: A numerical model to compute catchment-scale hydrologic transport using StorAge Selection functions. *Geoscientific Model Development*, *11*(4), 1627–1639. https://doi.org/10.5194/gmd-11-1627-2018

Benettin, P., Queloz, P., Bensimon, M., McDonnell, J. J., & Rinaldo, A. (2019). Velocities, residence times, tracer breakthroughs in a vegetated lysimeter: A multitracer experiment. *Water Resources Research*, *55*(1), 21–33. https://doi.org/10.1029/2018wr023894

Benettin, P., Soulsby, C., Birkel, C., Tetzlaff, D., Botter, G., & Rinaldo, A. (2017). Using SAS functions and high-resolution isotope data to unravel travel time distributions in headwater catchments. *Water Resources Research*, *53*(3), 1864–1878. https://doi.org/10.1002/2016WR020117

Berghuijs, W. R., & Kirchner, J. W. (2017). The relationship between contrasting ages of groundwater and streamflow. *Geophysical Research Letters*, *44*(17), 8925–8935. https://doi.org/10.1002/2017GL074962

Berkowitz, B., Cortis, A., Dentz, M., & Scher, H. (2006). Modeling non-fickian transport in geological formations as a continuous time random walk. *Reviews of Geophysics*, *44*(2), RG2003. https://doi.org/10.1029/2005RG000178

Berman, E. S. F., Gupta, M., Gabrielli, C., Garland, T., & McDonnell, J. J. (2009). High-frequency field-deployable isotope analyzer for hydrological applications. *Water Resources Research*, *45*(10), W10201. https://doi.org/10.1029/2009WR008265

Bertuzzo, E., Thomet, M., Botter, G., & Rinaldo, A. (2013). Catchment-scale herbicides transport: Theory and application. *Advances in Water Resources*, *52*, 232–242. https://doi.org/10.1016/j.advwatres.2012.11.007

Birkel, C., Soulsby, C., & Tetzlaff, D. (2011). Modelling catchment-scale water storage dynamics: Reconciling dynamic storage with tracer-inferred passive storage. *Hydrological Processes*, *25*(25), 3924–3936. https://doi.org/10.1002/hyp.8201

Botter, G., Bertuzzo, E., Bellin, A., & Rinaldo, A. (2005). On the Lagrangian formulations of reactive solute transport in the hydrologic response. *Water Resources Research*, *41*(4), W04008. https://doi.org/10.1029/2004WR003544

Botter, G., Bertuzzo, E., & Rinaldo, A. (2010). Transport in the hydrologic response: Travel time distributions, soil moisture dynamics, and the old water paradox. *Water Resources Research*, *46*, W03514. https://doi.org/10.1029/2009WR008371

Botter, G., Bertuzzo, E., & Rinaldo, A. (2011). Catchment residence and travel time distributions: The master equation. *Geophysical Research Letters*, *38*, L11403. https://doi.org/10.1029/2011GL047666

Bras, R. L. (2015). Complexity and organization in hydrology: A personal view. *Water Resources Research*, *51*(8), 6532–6548. https://doi.org/10.1002/2015WR016958

Christophersen, N., Neal, C., Hooper, R. P., Vogt, R. D., & Andersen, S. (1990). Modelling streamwater chemistry as a mixture of soilwater end-members - a step towards second-generation acidification models. *Journal of Hydrology*, *116*(1), 307–320. https://doi.org/10.1016/0022-1694(90)90130-P

Cirpka, O. A., Fienen, M. N., Hofer, M., Hoehn, E., Tessarini, A., Kipfer, R., & Kitanidis, P. K. (2007). Analyzing bank filtration by deconvoluting time series of electric conductivity. *Groundwater*, *45*(3), 318–328. https://doi.org/10.1111/j.1745-6584.2006.00293.x

Clark, M. P., Bierkens, M. F. P., Samaniego, L., Woods, R. A., Uijlenhoet, R., Bennett, K. E., … Peters-Lidard, C. D. (2017). The evolution of process-based hydrologic models: Historical challenges and the collective quest for physical realism. *Hydrology and Earth System Sciences*, *21*(7), 3427–3440. https://doi.org/10.5194/hess-21-3427-2017

Clymans, W., Govers, G., Frot, E., Ronchi, B., Van Wesemael, B., & Struyf, E. (2013). Temporal dynamics of bio-available Si fluxes in a temperate forested catchment (Meerdaal Forest, Belgium). *Biogeochemistry*, *116*(1–3), 275–291. https://doi.org/10.1007/s10533-013-9858-9

Correa, A., Windhorst, D., Tetzlaff, D., Crespo, P., Célleri, R., Feyen, J., & Breuer, L. (2017). Temporal dynamics in dominant runoff sources and flow paths in the andean páramo. *Water Resources Research*, *53*(7), 5998–6017. https://doi.org/10.1002/2016WR020187

Curtiss, J. H. (1941). On the distribution of the quotient of two chance variables. *Ann Math Stat*, *12*(4), 409–421. https://doi.org/10.1214/aoms/1177731679

Cvetkovic, V., Carstens, C., Selroos, J.-O., & Destouni, G. (2012). Water and solute transport along hydrological pathways. *Water Resources Research*, *48*(6), W06537. https://doi.org/10.1029/2011WR011367

Danesh-Yazdi, M., Botter, G., & Foufoula-Georgiou, E. (2017). Time-variant lagrangian transport formulation reduces aggregation bias of water and solute mean travel time in heterogeneous catchments. *Geophysical Research Letters*, *44*(10), 4880–4888. https://doi.org/10.1002/2017GL073827

Danesh-Yazdi, M., Klaus, J., Condon, L. E., & Maxwell, R. M. (2018). Bridging the gap between numerical solutions of travel time distributions and analytical StorAge Selection functions. *Hydrological Processes*, *32*(8), 1063–1076. https://doi.org/10.1002/hyp.11481

Davies, J., Beven, K., Rodhe, A., Nyberg, L., & Bishop, K. (2013). Integrated modeling of flow and residence times at the catchment scale with multiple interacting pathways. *Water Resources Research*, *49*(August), 4738–4750. https://doi.org/10.1002/wrcr.20377

Delavau, C. J., Stadnyk, T., & Holmes, T. (2017). Examining the impacts of precipitation isotope input ($\delta^{18}O^{ppt}$) on distributed, tracer-aided hydrological modelling. *Hydrology and Earth System Sciences*, *21*(5), 2595–2614. https://doi.org/10.5194/hess-21-2595-2017

Desbarats, A. J. (1990). Macrodispersion in sand-shale sequences. *Water Resources Research*, *26*(1), 153–163. https://doi.org/10.1029/WR026i001p00153

Dooge, J. C. I. (1986). Looking for hydrologic laws. *Water Resources Research*, *22*(9S), 46S–58S. https://doi.org/10.1029/WR022i09Sp0046S

Duy, N. L., Dung, N. V., Heidbüchel, I., Meyer, H., Weiler, M., Merz, B., & Apel, H. (2019). Identification of groundwater mean transit times of precipitation and riverbank infiltration by two-component lumped parameter models. *Hydrological Processes*, *33*, 3098–3118. https://doi.org/10.1002/hyp.13549

Eberts, S. M., Böhlke, J. K., Kauffman, L. J., & Jurgens, B. C. (2012). Comparison of particle-tracking and lumped-parameter age-distribution models for evaluating vulnerability of production wells to contamination. *Hydrogeology Journal*, *20*(2), 263–282. https://doi.org/10.1007/s10040-011-0810-6

Engdahl, N. B., & Maxwell, R. M. (2014). Approximating groundwater age distributions using simple streamtube models and multiple tracers. *Advances in Water Resources*, *66*, 19–31. https://doi.org/10.1016/j.advwatres.2014.02.001

Evaristo, J., Kim, M., van Haren, J., Pangle, L. A., Harman, C. J., Troch, P. A., & McDonnell, J. J. (2019). Characterizing the fluxes and age distribution of soil water, plant water, and deep percolation in a model tropical ecosystem. *Water Resources Research*, *55*(4), 3307–3327. https://doi.org/10.1029/2018WR023265

Glaser, B., Jackisch, C., Hopp, L., & Klaus, J. (2019). How meaningful are plot-scale observations and simulations of preferential flow for catchment models? *Vadose Zone Journal*, *18*(1), 1–18. https://doi.org/10.2136/vzj2018.08.0146

Goderniaux, P., Davy, P., Bresciani, E., de Dreuzy, J.-R., & Le Borgne, T. (2013). Partitioning a regional groundwater flow system into shallow local and deep regional flow compartments. *Water Resources Research*, *49*(4), 2274–2286. https://doi.org/10.1002/wrcr.20186

Gooseff, M. N., Benson, D. A., Briggs, M. A., Weaver, M., Wollheim, W., Peterson, B., & Hopkinson, C. S. (2011). Residence time distributions in surface transient storage zones in streams: Estimation via signal deconvolution. *Water Resources Research*, *47*(5), W05509. https://doi.org/10.1029/2010WR009959

Groh, J., Stumpp, C., Lücke, A., Pütz, T., Vanderborght, J., & Vereecken, H. (2018). Inverse estimation of soil hydraulic and transport parameters of layered soils from water stable isotope and lysimeter data. *Vadose Zone Journal*, *17*(1), 1–19. https://doi.org/10.2136/vzj2017.09.0168

Guillet, G., Knapp, J. L., Merel, S., Cirpka, O. A., Grathwohl, P., Zwiener, C., & Schwientek, M. (2019). Fate of wastewater contaminants in rivers: Using conservative-tracer based transfer functions to assess reactive transport. *Science of the Total Environment*, *656*, 1250–1260. https://doi.org/10.1016/j.scitotenv.2018.11.379

Gupta, P., Noone, D., Galewsky, J., Sweeney, C., & Vaughn, B. H. (2009). Demonstration of high-precision continuous measurements of water vapor isotopologues in laboratory and remote field deployments using wavelength-scanned cavity ring-down spectroscopy (ws-crds) technology. *Rapid Communications in Mass Spectrometry*, *23*(16), 2534–2542. https://doi.org/10.1002/rcm.4100

Haggerty, R., Wondzell, S. M., & Johnson, M. A. (2002). Power-law residence time distribution in the hyporheic zone of a 2nd-order mountain stream. *Geophysical Research Letters*, *29*(13), 18–1–18–4. https://doi.org/10.1029/2002GL014743

Harman, C. J. (2015). Time-variable transit time distributions and transport: Theory and application to storage-dependent transport of chloride in a watershed. *Water Resources Research*, *51*(1), 1–30. https://doi.org/10.1002/2014WR015707

Herbstritt, B., Gralher, B., & Weiler, M. (2019). Continuous, near-real-time observations of water stable isotope ratios during rainfall and throughfall events. *Hydrology and Earth System Sciences*, *23*(7), 3007–3019. https://doi.org/10.5194/hess-23-3007-2019

Hissler, C., Stille, P., Guignard, C., Iffly, J. F., & Pfister, L. (2014). Rare earth elements as hydrological tracers of anthropogenic and critical zone contributions: A case study at the Alzette river Basin scale. *Procedia Earth and Planetary Science*, *10*, 349–352. https://doi.org/10.1016/j.proeps.2014.08.036

Hornberger, G., Scanlon, T., & Raffensperger, J. (2001). Modelling transport of dissolved silica in a forested headwater catchment: The effect of hydrological and chemical time scales on hysteresis in the concentration-discharge relationship. *Hydrological Processes*, *15*(10), 2029–2038. https://doi.org/10.1002/hyp.254

Hrachowitz, M., Benettin, P., Breukelen, B. M. V., Fovet, O., Howden, N. J. K., Ruiz, L., … Wade, A. J. (2016). Transit times - the link between hydrology and water quality at the catchment scale. *Interdisciplinary Reviews: Water*, *3*, 629–657. https://doi.org/10.1002/wat2.1155

Hrachowitz, M., & Clark, M. P. (2017). Hess opinions: The complementary merits of competing modelling philosophies in hydrology. *Hydrology and Earth System Sciences*, *21*(8), 3953–3973. https://doi.org/10.5194/hess-21-3953-2017

Hrachowitz, M., Soulsby, C., Tetzlaff, D., Dawson, J., Dunn, S., & Malcolm, I. (2009). Using long-term data sets to understand transit times in contrasting headwater catchments. *Journal of Hydrology*, *367*(3), 237–248. https://doi.org/10.1016/j.jhydrol.2009.01.001

Hrachowitz, M., Soulsby, C., Tetzlaff, D., & Malcolm, I. A. (2011). Sensitivity of mean transit time estimates to model conditioning and data availability. *Hydrological Processes*, *25*(6), 980–990. https://doi.org/10.1002/hyp.7922

IAEA (2019). Global network of isotopes in rivers: The GNIR database.

IAEA & WMO (2019). Global network of isotopes in precipitation: The GNIP database.

Jackisch, C., Angermann, L., Allroggen, N., Sprenger, M., Blume, T., Tronicke, J., & Zehe, E. (2017). Form and function in hillslope hydrology: In situ imaging and characterization of flow-relevant structures. *Hydrology and Earth System Sciences*, *21*(7), 3749–3775. https://doi.org/10.5194/hess-21-3749-2017

Jing, M., Heße, F., Kumar, R., Kolditz, O., Kalbacher, T., & Attinger, S. (2019). Influence of input and parameter uncertainty on the prediction of catchment-scale groundwater travel time distributions. *Hydrology and Earth System Sciences*, *23*(1), 171–190. https://doi.org/10.5194/hess-23-171-2019

Johnson, N. M., Likens, G. E., Bormann, F., & Pierce, R. S. (1968). Rate of chemical weathering of silicate minerals in New Hampshire. *Geochimica et Cosmochimica Acta*, *32*(5), 531–545. https://doi.org/10.1016/0016-7037(68)90044-6

Kaandorp, V. P., de Louw, P. G. B., vander Velde, Y., & Broers, H. P. (2018). Transient groundwater travel time distributions and age-ranked storage-discharge relationships of three lowland catchments. *Water Resources Research*, *54*(7), 4519–4536. https://doi.org/10.1029/2017wr022461

Kendall, C., McDonnell, J. J., & Gu, W. (2001). A look inside 'black box' hydrograph separation models: A study at the hydrohill catchment. *Hydrological Processes*, *15*(10), 1877–1902. https://doi.org/10.1002/hyp.245

Kim, M., Pangle, L. A., Cardoso, C., Lora, M., Volkmann, T. H. M., Wang, Y., … Troch, P. A. (2016). Transit time distributions and StorAge Selection functions in a sloping soil lysimeter with time-varying flow paths: Direct observation of internal and external transport variability. *Water Resources Research.*, *52*, 7105–7129. https://doi.org/10.1002/2016WR018620

Kirchner, J. W. (2016). Aggregation in environmental systems - part 1: Seasonal tracer cycles quantify young water fractions, but not mean transit times, in spatially heterogeneous catchments. *Hydrology and Earth System Sciences*, *20*(1), 279–297. https://doi.org/10.5194/hess-20-279-2016

Kirchner, J. W. (2019). Quantifying new water fractions and transit time distributions using ensemble hydrograph separation: Theory and benchmark tests. *Hydrology and Earth System Sciences*, *23*(1), 303–349. https://doi.org/10.5194/hess-23-303-2019

Kirchner, J. W., Feng, X., & Neal, C. (2000). Fractal stream chemistry and its implications for contaminant transport in catchments. *Nature*, *403*(6769), 524–527. https://doi.org/10.1038/35000537

Kirchner, J. W., Feng, X., & Neal, C. (2001). Catchment-scale advection and dispersion as a mechanism for fractal scaling in stream tracer concentrations. *Journal of Hydrology*, *254*(1–4), 82–101. https://doi.org/10.1016/S0022-1694(01)00487-5

Kirchner, J. W., Feng, X., Neal, C., & Robson, A. J. (2004). The fine structure of water-quality dynamics: The (high-frequency) wave of the future. *Hydrological Processes*, *18*(7), 1353–1359. https://doi.org/10.1002/hyp.5537

Kirchner, J. W., & Neal, C. (2013). Universal fractal scaling in stream chemistry and its implications for solute transport and water quality trend detection. *Proceedings of the National Academy of Sciences of the United States of America*, *110*(30), 12213–12218. https://doi.org/10.1073/pnas.1304328110

Klaus, J., Zehe, E., Elsner, M., Külls, C., & McDonnell, J. J. (2013). Macropore flow of old water revisited: Experimental insights from a tile-drained hillslope. *Hydrology and Earth System Sciences*, *17*(1), 103–118. https://doi.org/10.5194/hess-17-103-2013

Koehler, G. & Wassenaar, L. I. (2011). Realtime stable isotope monitoring of natural waters by parallel-flow laser spectroscopy. *Analytical Chemistry*, *83*(3), 913–919. PMID: 21214188. doi:https://doi.org/10.1021/ac102584q.

Kreft, A., & Zuber, A. (1978). On the physical meaning of the dispersion equation and its solutions for different initial and boundary conditions. *Chemical Engineering Science*, *33*(11), 1471–1480. https://doi.org/10.1016/0009-2509(78)85196-3

Le Borgne, T., de Dreuzy, J.-R., Davy, P., & Bour, O. (2007). Characterization of the velocity field organization in heterogeneous media by conditional correlation. *Water Resources Research*, *43*(2), W02419. https://doi.org/10.1029/2006WR004875

Leray, S., Engdahl, N. B., Massoudieh, A., Bresciani, E., & McCallum, J. (2016). Residence time distributions for hydrologic systems: Mechanistic foundations and steady-state analytical solutions. *Journal of Hydrology*, *543*, 67–87. https://doi.org/10.1016/j.jhydrol.2016.01.068

Lis, G., Wassenaar, L. I., & Hendry, M. J. (2008). High-precision laser spectroscopy d/h and 18o/16o measurements of microliter natural water samples. *Analytical Chemistry*, *80*(1), 287–293. PMID: 18031060. doi: https://doi.org/10.1021/ac701716q.

Long, A. J., & Putnam, L. D. (2009). Age-distribution estimation for karst groundwater: Issues of parameterization and complexity in inverse modeling by convolution. *Journal of Hydrology*, *376*(3), 579–588. https://doi.org/10.1016/j.jhydrol.2009.07.064

Luo, J., & Cirpka, O. A. (2008). Traveltime-based descriptions of transport and mixing in heterogeneous domains. *Water Resources Research*, *44* (9), W09407. https://doi.org/10.1029/2007WR006035

Maher, K. (2010). The dependence of chemical weathering rates on fluid residence time. *Earth and Planetary Science Letters*, *294*(1–2), 101–110. https://doi.org/10.1016/j.epsl.2010.03.010

Maher, K. (2011). The role of fluid residence time and topographic scales in determining chemical fluxes from landscapes. *Earth and Planetary Science Letters*, *312*, 48–58. https://doi.org/10.1016/j.epsl.2011.09.040

Maher, K., & Chamberlain, C. P. (2014). Hydrologic regulation of chemical weathering and the geologic carbon cycle. *Science*, *343*(6178), 1502–1504. https://doi.org/10.1126/science.1250770

Małoszewski, P., & Zuber, A. (1982). Determining the turnover time of groundwater systems with the aid of environmental tracers: 1. Models and their applicability. *Journal of Hydrology*, *57*(3), 207–231. https://doi.org/10.1016/0022-1694(82)90147-0

Martinez-Carreras, N., Wetzel, C. E., Frentress, J., Ector, L., McDonnell, J. J., Hoffmann, L., & Pfister, L. (2015). Hydrological connectivity inferred from diatom transport through the riparian-stream system. *Hydrology and Earth System Sciences*, *19*(7), 3133–3151. https://doi.org/10.5194/hess-19-3133-2015

Massoudieh, A., Sharifi, S., & Solomon, D. K. (2012). Bayesian evaluation of groundwater age distribution using radioactive tracers and anthropogenic chemicals. *Water Resources Research*, *48*(9), W09529. https://doi.org/10.1029/2012WR011815

Massoudieh, A., Visser, A., Sharifi, S., & Broers, H. P. (2014). A bayesian modeling approach for estimation of a shape-free groundwater age distribution using multiple tracers. *Applied Geochemistry*, *50*, 252–264. https://doi.org/10.1016/j.apgeochem.2013.10.004

Maxwell, R. M., Condon, L. E., Danesh-Yazdi, M., & Bearup, L. A. (2018). Exploring source water mixing and transient residence time distributions of outflow and evapotranspiration with an integrated hydrologic model and lagrangian particle tracking approach. *Ecohydrology*, *12*(1), e2042. https://doi.org/10.1002/eco.2042

McCallum, J. L., Engdahl, N. B., Ginn, T. R., & Cook, P. G. (2014). Nonparametric estimation of groundwater residence time distributions: What can environmental tracer data tell us about groundwater residence time? *Water Resources Research*, *50*(3), 2022–2038. https://doi.org/10.1002/2013WR014974

McDonnell, J. J., & Beven, K. J. (2014). Debates on water resources: The future of hydrological sciences: A (common) path forward? A call to action aimed at understanding velocities, celerities and residence time distributions of the headwater hydrograph. *Water Resources Research*, *50*(6), 5342–5350. https://doi.org/10.1002/2013WR015141

McGuire, K. J., & McDonnell, J. J. (2006). A review and evaluation of catchment transit time modeling. *Journal of Hydrology*, *330*(3–4), 543–563. https://doi.org/10.1016/j.jhydrol.2006.04.020

Munksgaard, N. C., Wurster, C. M., & Bird, M. I. (2011). Continuous analysis of $\delta^{18}O$ and δD values of water by diffusion sampling cavity ring-down spectrometry: A novel sampling device for unattended field monitoring of precipitation, ground and surface waters. *Rapid Communications in Mass Spectrometry*, *25*(24), 3706–3712. https://doi.org/10.1002/rcm.5282

Neal, C., Reynolds, B., Kirchner, J. W., Rowland, P., Norris, D., Sleep, D., … Armstrong, L. (2013). High-frequency precipitation and stream water quality time series from Plynlimon, Wales: An openly accessible data resource spanning the periodic table. *Hydrological Processes*, *27*(17), 2531–2539. https://doi.org/10.1002/hyp.9814

Neal, C., Reynolds, B., Norris, D., Kirchner, J. W., Neal, M., Rowland, P., … Wright, D. (2011). Three decades of water quality measurements from the upper Severn experimental catchments at Plynlimon, Wales: An openly accessible data resource for research, modelling, environmental management and education. *Hydrological Processes*, *25*(24), 3818–3830. https://doi.org/10.1002/hyp.8191

Oldham, C. E., Farrow, D. E., & Peiffer, S. (2013). A generalized damkohler number for classifying material processing in hydrological systems. *Hydrology and Earth System Sciences*, *17*(3), 1133–1148. https://doi.org/10.5194/hess-17-1133-2013

Pangle, L. A., Kim, M., Cardoso, C., Lora, M., Meira Neto, A. A., Volkmann, T. H. M., … Harman, C. J. (2017). The mechanistic basis for storage-dependent age distributions of water discharged from an experimental hillslope. *Water Resources Research*, *53*(4), 2733–2754. https://doi.org/10.1002/2016WR019901

Pangle, L. A., Klaus, J., Berman, E. S. F., Gupta, M., & McDonnell, J. J. (2013). A new multisource and high-frequency approach to measuring δ^2H in hydrological field studies. *Water Resources Research*, *49*(11), 7797–7803. https://doi.org/10.1002/2013WR013743

Parnell, A. C., Phillips, D. L., Bearhop, S., Semmens, B. X., Ward, E. J., Moore, J. W., … Inger, R. (2013). Bayesian stable isotope mixing models. *Environmetrics*, *24*(6), 387–399. https://doi.org/10.1002/env.2221

Pfister, L., Martínez-Carreras, N., Hissler, C., Klaus, J., Carrer, G. E., Stewart, M. K., & McDonnell, J. J. (2017). Bedrock geology controls on catchment storage, mixing, and release: A comparative analysis of 16 nested catchments. *Hydrological Processes*, *31*(10), 1828–1845. https://doi.org/10.1002/hyp.11134

Pfister, L., Wetzel, C. E., Klaus, J., Martínez-Carreras, N., Antonelli, M., Teuling, A. J., & McDonnell, J. J. (2017). Terrestrial diatoms as tracers in catchment hydrology: A review. *Wiley Interdisciplinary Reviews: Water*, *4*(6), e1241. https://doi.org/10.1002/wat2.1241

Pütz, T., Kiese, R., Wollschläger, U., Groh, J., Rupp, H., Zacharias, S., … Vereecken, H. (2016). Tereno-soilcan: A lysimeter-network in Germany observing soil processes and plant diversity influenced by climate change. *Environmental Earth Sciences*, *75*(18), 1242. https://doi.org/10.1007/s12665-016-6031-5

Queloz, P., Bertuzzo, E., Carraro, L., Botter, G., Miglietta, F., Rao, P., & Rinaldo, A. (2015). Transport of fluorobenzoate tracers in a vegetated hydrologic control volume: 1. Experimental results. *Water Resources Research*, *51*(4), 2773–2792. https://doi.org/10.1002/2014WR016433

Queloz, P., Carraro, L., Benettin, P., Botter, G., Rinaldo, A., & Bertuzzo, E. (2015). Transport of fluorobenzoate tracers in a vegetated hydrologic control volume: 2. Theoretical inferences and modeling. *Water Resources Research*, *51*(4), 2793–2806. https://doi.org/10.1002/2014WR016508

Remondi, F., Kirchner, J. W., Burlando, P., & Fatichi, S. (2018). Water flux tracking with a distributed hydrological model to quantify controls on the spatiotemporal variability of transit time distributions. *Water Resources Research*, *54*(4), 3081–3099. https://doi.org/10.1002/2017wr021689

Rinaldo, A., Benettin, P., Harman, C. J., Hrachowitz, M., McGuire, K. J., van der Velde, Y., … Botter, G. (2015). StorAge Selection functions: A coherent framework for quantifying how catchments store and release water and solutes. *Water Resources Research*, *51*(6), 4840–4847. https://doi.org/10.1002/2015WR017273

Rinaldo, A., & Marani, A. (1987). Basin scale-model of solute transport. *Water Resources Research*, *23*(11), 2107–2118. https://doi.org/10.1029/WR023i011p02107

Rinaldo, A., Marani, A., & Rigon, R. (1991). Geomorphological dispersion. *Water Resources Research*, *27*(4), 513–525.

Rinaldo, A., Vodel, G., Rigon, R., & Rodriguez-Iturbe, I. (1995). Can one gauge the shape of a basin? *Water Resources Research*, *31*(4), 1119–1127. https://doi.org/10.1029/94WR03290

Ritzi, R. W., Dominic, D. F., Slesers, A. J., Greer, C. B., Reboulet, E. C., Telford, J. A., … Means, B. P. (2000). Comparing statistical models of physical heterogeneity in buried-valley aquifers. *Water Resources Research*, *36*(11), 3179–3192. https://doi.org/10.1029/2000WR900143

Rodhe, A., Nyberg, L., & Bishop, K. (1996). Transit times for water in a small till catchment from a step shift in the oxygen 18 content of the water input. *Water Resources Research*, *32*(12), 3497–3511. https://doi.org/10.1029/95WR01806

Rodriguez, N. B., & Klaus, J. (2019). Catchment travel times from composite StorAge Selection functions representing the superposition of streamflow generation processes. *Water Resources Research*, *55*(11), 9292–9314. https://doi.org/10.1029/2019WR024973

Rodriguez, N. B., McGuire, K. J., & Klaus, J. (2018). Time-varying storage-water age relationships in a catchment with a mediterranean climate. *Water Resources Research*, *54*(6), 3988–4008. https://doi.org/10.1029/2017wr021964

Rodriguez, N. B., Pfister, L., Zehe, E., & Klaus, J. (2019). Testing the truncation of travel times with StorAge Selection functions using deuterium and tritium as tracers. *Hydrology and Earth System Sciences Discussions*, *2019*, 1–37. https://doi.org/10.5194/hess-2019-501

Rodriguez-Iturbe, I., & Valdes, J. B. (1979). The geomorphologic structure of hydrologic response. *Water Resources Research*, *15*(6), 1409–1420. https://doi.org/10.1029/WR015i006p01409

Sayama, T., & McDonnell, J. J. (2009). A new time-space accounting scheme to predict stream water residence time and hydrograph source components at the watershed scale. *Water Resources Research*, *45*(7), W07401. https://doi.org/10.1029/2008WR007549

Scaini, A., Amvrosiadi, N., Hissler, C., Pfister, L., & Beven, K. (2019). Following tracer through the unsaturated zone using a multiple interacting pathways model: Implications from laboratory experiments. *Hydrological Processes*, *33*, 2300–2313. https://doi.org/10.1002/hyp.13466

Scaini, A., Audebert, M., Hissler, C., Fenicia, F., Gourdol, L., Pfister, L., & Beven, K. J. (2017). Velocity and celerity dynamics at plot scale inferred from artificial tracing experiments and time-lapse ert. *Journal of Hydrology*, *546*, 28–43. https://doi.org/10.1016/j.jhydrol.2016.12.035

Seibert, J. & McDonnell, J. J. (2002). On the dialog between experimentalist and modeler in catchment hydrology: Use of soft data for multicriteria model calibration. *Water Resources Research*, *38*(11), 1241. doi:https://doi.org/10.1029/2001WR000978.

Smith, A. A., Tetzlaff, D., & Soulsby, C. (2018). On the use of StorAge Selection functions to assess time-variant travel times in lakes. *Water Resources Research*, *54*(7), 5163–5185. https://doi.org/10.1029/2017wr021242

Solomon, D. K., Genereux, D. P., Plummer, L. N., & Busenberg, E. (2010). Testing mixing models of old and young groundwater in a tropical lowland rain forest with environmental tracers. *Water Resources Research*, *46*(4), W04518. https://doi.org/10.1029/2009WR008341

Soulsby, C., Birkel, C., Geris, J., & Tetzlaff, D. (2015). Spatial aggregation of time-variant stream water ages in urbanizing catchments. *Hydrological Processes*, *29*(13), 3038–3050. https://doi.org/10.1002/hyp.10500

Sternagel, A., Loritz, R., Wilcke, W., & Zehe, E. (2019). Simulating preferential soil water flow and tracer transport using the Lagrangian soil water and solute transport model. *Hydrology and Earth System Sciences Discussions*, *2019*, 1–25. https://doi.org/10.5194/hess-2019-132

Stewart, M. K., Morgenstern, U., & McDonnell, J. J. (2010). Truncation of stream residence time: How the use of stable isotopes has skewed our concept of streamwater age and origin. *Hydrological Processes*, *24*(12), 1646–1659. https://doi.org/10.1002/hyp.7576

Stockinger, M. P., Bogena, H. R., Lücke, A., Diekkrüger, B., Cornelissen, T., & Vereecken, H. (2016). Tracer sampling frequency influences estimates of young water fraction and streamwater transit time distribution. *Journal of Hydrology*, *541*, 952–964. https://doi.org/10.1016/j.jhydrol.2016.08.007

Stolp, B. J., Solomon, D. K., Suckow, A., Vitvar, T., Rank, D., Aggarwal, P. K., & Han, L. F. (2010). Age dating base flow at springs and gaining streams using helium-3 and tritium: Fischa-dagnitz system, Southern Vienna basin, Austria. *Water Resources Research*, *46*(7), W07503. https://doi.org/10.1029/2009WR008006

Stumpp, C., Nützmann, G., Maciejewski, S., & Maloszewski, P. (2009). A comparative modeling study of a dual tracer experiment in a large lysimeter under atmospheric conditions. *Journal of Hydrology*, *375*(3–4), 566–577. https://doi.org/10.1016/j.jhydrol.2009.07.010

ter Braak, C. J. F., & Vrugt, J. A. (2008). Differential evolution Markov chain with snooker updater and fewer chains. *Statistics and Computing*, *18*(4), 435–446. https://doi.org/10.1007/s11222-008-9104-9

Turner, J. V., & Macpherson, D. K. (1990). Mechanisms affecting streamflow and stream water quality: An approach via stable isotope, hydrogeochemical,and time series analysis. *Water Resources Research*, *26*(12), 3005–3019. https://doi.org/10.1029/WR026i012p03005

Utermann, J., Kladivko, E. J., & Jury, W. A. (1990). Evaluating pesticide migration in tile-drained soils with a transfer function model. *Journal of Environmental Quality*, *19*, 707–714. doi:https://doi.org/10.2134/jeq1990.00472425001900040013x.

van der Velde, Y., Heidbüchel, I., Lyon, S. W., Nyberg, L., Rodhe, A., Bishop, K., & Troch, P. A. (2015). Consequences of mixing assumptions for time-variable travel time distributions. *Hydrological Processes*, *29*(16), 3460–3474. https://doi.org/10.1002/hyp.10372

van Huijgevoort, M. H. J., Tetzlaff, D., Sutanudjaja, E. H., & Soulsby, C. (2016). Using high resolution tracer data to constrain water storage, flux and age estimates in a spatially distributed rainfall-runoff model. *Hydrological Processes*, *Pages n/a–n/a.*, *30*, 4761–4778. https://doi.org/10.1002/hyp.10902

van Meerveld, H. J. I., Kirchner, J. W., Vis, M. J. P., Assendelft, R. S., & Seibert, J. (2019). Expansion and contraction of the flowing stream network alter hillslope flowpath lengths and the shape of the travel time distribution. *Hydrology and Earth System Sciences*, *23*(11), 4825–4834. https://doi.org/10.5194/hess-23-4825-2019

van Schaik, N. L. M. B., Bronstert, A., de Jong, S. M., Jetten, V. G., van Dam, J. C., Ritsema, C. J., & Schnabel, S. (2014). Process-based modelling of a headwater catchment in a semi-arid area: The influence of macropore flow. *Hydrological Processes*, *28*(24), 5805–5816. https://doi.org/10.1002/hyp.10086

vander Velde, Y., de Rooij, G. H., Rozemeijer, J. C., van Geer, F. C., & Broers, H. P. (2010). Nitrate response of a lowland catchment: On the relation between stream concentration and travel time distribution dynamics. *Water Resources Research*, *46*, W11534. https://doi.org/10.1029/2010WR009105

vander Velde, Y., Torfs, P. J. J. F., vander Zee, S. E. A. T. M., & Uijlenhoet, R. (2012). Quantifying catchment-scale mixing and its effect on time-varying travel time distributions. *Water Resources Research*, *48*, W06536. https://doi.org/10.1029/2011WR011310

Visser, A., Broers, H. P., Purtschert, R., Sültenfuß, J., & de Jonge, M. (2013). Groundwater age distributions at a public drinking water supply well field derived from multiple age tracers (85kr, 3h/3he, and 39ar). *Water Resources Research*, *49*(11), 7778–7796. https://doi.org/10.1002/2013WR014012

Visser, A., Thaw, M., Deinhart, A., Bibby, R., Safeeq, M., Conklin, M., … Van der Velde, Y. (2019). Cosmogenic isotopes unravel the hydrochronology and water storage dynamics of the Southern Sierra critical Zone. *Water Resources Research*, *55*(2), 1429–1450. https://doi.org/10.1029/2018WR023665

Volkmann, T. H. M., Sengupta, A., Pangle, L. A., Dontsova, K., Barron-Gafford, G. A., Harman, C. J., … Troch, P. A. (2018). Chapter 2: Controlled experiments of hillslope coevolution at the biosphere 2 landscape evolution observatory: Toward prediction of coupled hydrological, biogeochemical, and ecological change. In J.-F. Liu & W.-Z. Gu (Eds.), *Hydrology of Artificial and Controlled Experiments*. Rijeka, Croatia: IntechOpen.

von Freyberg, J., Studer, B., & Kirchner, J. W. (2017). A lab in the field: High-frequency analysis of water quality and stable isotopes in stream water and precipitation. *Hydrology and Earth System Sciences*, *21*(3), 1721–1739. https://doi.org/10.5194/hess-21-1721-2017

von Freyberg, J., Studer, B., Rinderer, M., & Kirchner, J. W. (2018). Studying catchment storm response using event- and pre-event-water volumes as fractions of precipitation rather than discharge. *Hydrology and Earth System Sciences*, *22*(11), 5847–5865. https://doi.org/10.5194/hess-22-5847-2018

Vrugt, J., Braak, C. T., Diks, C., Robinson, B., Hyman, J., & Higdon, D. (2009). Accelerating Markov chain Monte Carlo simulation by differential evolution with self-adaptive randomized subspace sampling. *International Journal of Nonlinear Sciences & Numerical Simulation*, *10*(3), 271–288. https://doi.org/10.1515/IJNSNS.2009.10.3.273

Ward, A. S., Schmadel, N. M., & Wondzell, S. M. (2018). Time-variable transit time distributions in the hyporheic zone of a headwater mountain stream. *Water Resources Research*, *54*(3), 2017–2036. https://doi.org/10.1002/2017WR021502

Weissmann, G. S., Zhang, Y., LaBolle, E. M., & Fogg, G. E. (2002). Dispersion of groundwater age in an alluvial aquifer system. *Water Resources Research*, *38*(10), 16–1–16–13. doi:https://doi.org/10.1029/2001WR000907.

White, R. E., Dyson, J. S., Haigh, R. A., Jury, W. A., & Sposito, G. (1986). A transfer function model of solute transport through soil: 2. Illustrative applications. *Water Resources Research*, *22*(2), 248–254. https://doi.org/10.1029/WR022i002p00248

Wilusz, D., Harman, C., Ball, W., Maxwell, R., & Buda, A. (2020). Using particle tracking to understand flow paths, age distributions, and the paradoxical origins of the inverse storage effect in an experimental catchment. *Water Resources Research*, *55*, e24397. https://doi.org/10.1029/2019WR025140

Wilusz, D. C., Harman, C. J., & Ball, W. P. (2017). Sensitivity of catchment transit times to rainfall variability under present and future climates. *Water Resources Research. In Press.*, *53*, 10231–10256. https://doi.org/10.1002/2017WR020894

Yang, J., Heidbüchel, I., Musolff, A., Reinstorf, F., & Fleckenstein, J. H. (2018). Exploring the dynamics of transit times and subsurface mixing in a small agricultural catchment. *Water Resources Research*, *54*(3), 2317–2335. https://doi.org/10.1002/2017wr021896

Zehe, E., & Jackisch, C. (2016). A lagrangian model for soil water dynamics during rainfall-driven conditions. *Hydrology and Earth System Sciences*, *20*(9), 3511–3526. https://doi.org/10.5194/hess-20-3511-2016

Zhang, Z. Q., Evaristo, J., Li, Z., Si, B. C., & McDonnell, J. J. (2017). Tritium analysis shows apple trees may be transpiring water several decades old. *Hydrological Processes*, *31*(5), 1196–1201. https://doi.org/10.1002/hyp.11108

SUPPORTING INFORMATION

Additional supporting information may be found online in the Supporting Information section at the end of this article.

How to cite this article: Rodriguez NB, Benettin P, Klaus J. Multimodal water age distributions and the challenge of complex hydrological landscapes. *Hydrological Processes*. 2020; 1–18. https://doi.org/10.1002/hyp.13770